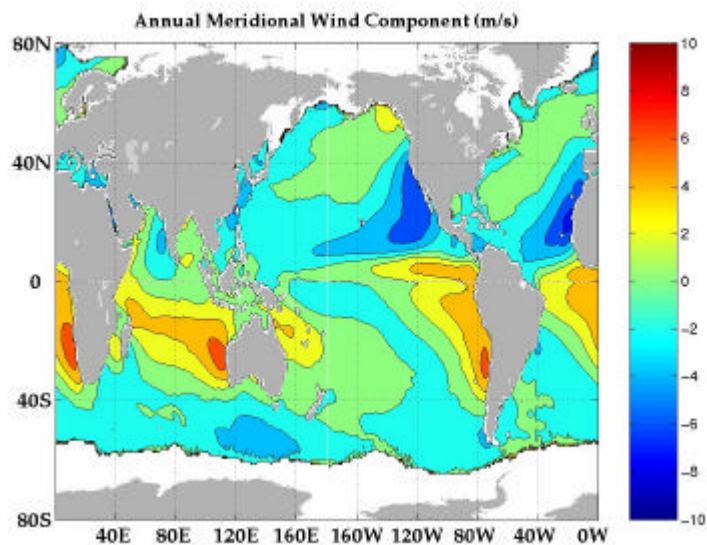
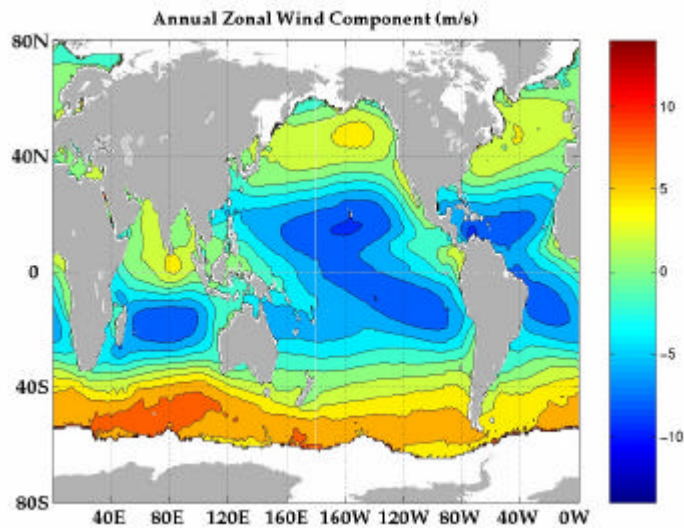


# **QUIKSCAT SCATTEROMETER MEAN WIND FIELD PRODUCTS USER MANUAL**

Réf. : C2-MUT-W-04-IF

Version : 1.0

Date : May 2002



## FOREWORD

The volume 2 of the MWF (**M**ean **W**ind **F**ields) product manual presents objectively analyzed fields of surface wind parameters. These gridded wind fields are computed from the individual observations provided by the NASA scatterometer SeaWinds onboard QuikSCAT. These raw data, supplied by JPL/PO.DAAC (Level 2B data), are analyzed on a 0.5 degree by 0.5 degree global grid over various averaging time period. The data, the method of analysis, the geophysical parameters and all information to read the mean wind fields are described, in some details, in this manual. Mean wind fields computed from ERS-1, ERS-2 and NSCAT on 1 x 1 degree grids are presented in volume 1 of this manual.

This work was performed and funded by IFREMER / CERSAT. We request that you furnish us with a copy of any publication employing these data and that the source of the data be acknowledged in the publication. As always, we welcome your suggestions and would welcome a visit, here at CERSAT whenever your travels allow it.

We thank the Physical Oceanography Distributed Active Archive Centre (PO.DAAC), which distributes the SeaWinds/QuikSCAT L2B Level data.

# TABLE OF CONTENTS

<b>TABLE OF CONTENTS .....</b>	<b>2</b>
<b>1. Introduction .....</b>	<b>4</b>
<b>1.1. Purpose.....</b>	<b>4</b>
<b>1.2. Product overview.....</b>	<b>4</b>
<b>1.3. User manual overview.....</b>	<b>4</b>
<b>2. The QuikSCAT mission.....</b>	<b>6</b>
<b>2.1. Mission Description.....</b>	<b>6</b>
<b>2.2. Satellite Description .....</b>	<b>7</b>
<b>2.3. SeaWinds Sensor Overview.....</b>	<b>7</b>
2.3.1. Introduction to QuikSCAT.....	8
2.3.2. Principles of Operation.....	8
<b>2.4. Retrieving wind vectors from scatterometer measurements.....</b>	<b>9</b>
<b>3. Processing details.....</b>	<b>11</b>
<b>3.1. Processing scheme .....</b>	<b>11</b>
<b>3.2. QuikSCAT Level 2B wind data selection.....</b>	<b>11</b>
<b>3.3. Wind stress estimation.....</b>	<b>12</b>
<b>3.4. Sampling .....</b>	<b>13</b>
<b>3.5. Estimation of gridded wind fields .....</b>	<b>14</b>
<b>3.6. Wind divergence and stress curl estimation.....</b>	<b>17</b>
<b>4. Product description.....</b>	<b>18</b>
<b>4.1. Main characteristics .....</b>	<b>18</b>
4.1.1. Spatial coverage .....	18
4.1.2. Spatial resolution.....	18
4.1.3. Grid description.....	18
4.1.4. Temporal coverage .....	18
4.1.5. Temporal resolution .....	18
4.1.6. Land mask .....	19
4.1.7. Ice mask.....	19
4.1.8. Main parameters .....	19
4.1.9. Storage .....	19
4.1.10. Data volume .....	19
4.1.11. Conventions .....	19
<b>4.2. Header structure .....</b>	<b>20</b>
4.2.1. WOCE_version .....	20
4.2.2. CONVENTIONS .....	20
4.2.3. long_name .....	20
4.2.4. short_name .....	20
4.2.5. producer_agency .....	21
4.2.6. producer_institution .....	21
4.2.7. netcdf_version_id .....	21
4.2.8. product_version.....	21
4.2.9. creation_time .....	21
4.2.10. start_date .....	21
4.2.11. stop_date.....	21
4.2.12. time_resolution.....	21
4.2.13. spatial_resolution .....	21
4.2.14. platform_id .....	22

4.2.15. instrument .....	22
4.2.16. objective_method .....	22
4.2.17. north_latitude .....	22
4.2.18. south_latitude .....	22
4.2.19. west_longitude .....	22
4.2.20. east_longitude.....	22
<b>4.3. Data structure .....</b>	<b>22</b>
4.3.1. time .....	23
4.3.2. depth.....	23
4.3.3. woce_date .....	23
4.3.4. woce_time_of_day.....	23
4.3.5. latitude .....	24
4.3.6. longitude .....	24
4.3.7. swath_count.....	24
4.3.8. quality_flag.....	24
4.3.9. wind_speed .....	25
4.3.10. wind_speed_error.....	25
4.3.11. zonal_wind_speed .....	25
4.3.12. zonal_wind_speed_error .....	26
4.3.13. meridional_wind_speed .....	26
4.3.14. meridional_wind_speed_error.....	26
4.3.15. wind_speed_divergence .....	26
4.3.16. wind_stress.....	27
4.3.17. wind_stress_error .....	27
4.3.18. zonal_wind_stress .....	27
4.3.19. zonal_wind_stress_error.....	27
4.3.20. meridional_wind_stress.....	28
4.3.21. meridional_wind_stress_error .....	28
4.3.22. wind_stress_curl.....	28
<b>5. Data use.....</b>	<b>29</b>
<b>5.1. Data access.....</b>	<b>29</b>
5.1.1. Ftp access .....	29
5.1.2. WWW access .....	29
5.1.3. On-line browser .....	29
<b>5.2. Reading the data.....</b>	<b>29</b>
<b>6. Validation &amp; accuracy .....</b>	<b>30</b>
<b>6.1. Introduction.....</b>	<b>30</b>
<b>6.2. Aliasing in regular wind fields .....</b>	<b>31</b>
<b>6.3. Comparison of surface winds from QuikSCAT and buoys.....</b>	<b>34</b>
<b>6.4. Validation of QuikSCat wind fields over global oceans .....</b>	<b>35</b>
<b>6.5. QuikSCAT Mean Wind Field Characteristics .....</b>	<b>37</b>
6.5.1. Wind Field .....	37
6.5.2. Wind Stress .....	39
6.5.3. Wind Divergence and Wind Stress Curl .....	41
<b>7. References.....</b>	<b>46</b>
<b>8. Contacts.....</b>	<b>47</b>

# 1. Introduction

CERSAT is the acronym for "Centre ERS d'Archivage et de Traitement", the French Processing and Archiving Facility for ERS-1 and ERS-2. For more information, check our Web site at :

<http://www.ifremer.fr/cersat/>

## 1.1. Purpose

Surface wind is a key parameter for the determination of many ocean-atmosphere interaction parameters such as air-sea latent and sensible heat fluxes and air-sea transfer rate of carbon dioxide, momentum flux and the wind stress on the surface layer of the ocean.

This product was intended to provide the scientific community with easy-to-use synoptic gridded fields of wind parameters as retrieved from ESA scatterometer AMI-Wind onboard ERS-1 & ERS-2, from NASA scatterometers NSCAT onboard ADEOS and SeaWinds onboard QuikSCAT. These mean wind fields make available a complete time series of global satellite wind fields over a 11 years long period.

This manual deals with the mean wind fields computed from QuikSCAT. The user should refer to volume 1 for the also available ERS-1, ERS-2 and NSCAT mean wind fields.

## 1.2. Product overview

The QuikSCAT MWF product provides daily, weekly and monthly wind fields over global  $0.5^\circ \times 0.5^\circ$  resolution geographical grids. Main parameters include wind speed (module, divergence and components), wind stress (magnitude, curl and components). In order to reconstruct gap-filled and averaged synoptic fields from discrete observations (available in JPL/PO.DAAC L2B product) over each time period, a statistical interpolation is performed using an objective method; the standard errors of the parameters estimated by this method are also computed and provided as complementary gridded fields. Wind divergence and stress curl are also derived respectively from wind and stress grids and included in the dataset.

## 1.3. User manual overview

This document gives a comprehensive description of data format and contents of QuikSCAT Mean Wind Fields (MWF) distributed by CERSAT. This manual also provides an overview of QuikSCAT mission, and comments on gridded fields accuracy together with the algorithm principles for QuikSCAT MWF processing. More information on QuikSCAT/SeaWinds raw data and sensors can be found in JPL project documents [1] [2].

Section 2 gives an overview of QuikSCAT mission, including a description of scatterometry principles, satellite, orbit & sensors characteristics. Most of the information provided in this section is issued from JPL/PO.DAAC QuikSCAT User's manual [1].

Section 3 describes the overall processing method.

Section 4 provides a description of CERSAT MWF product files (nomenclature, contents overview and format).

Section 5 explains how to access and use the data.

Section 6 provides information on gridded field validation and accuracy.

Section 7 includes a glossary and references, and gives points of contact for more information.

## 2. Measuring the wind with QuikSCAT

Part of this section is extracted from the JPL document 'QuikSCAT Science Data Product, User's Manual, Overview & Geophysical Data Products'. Version 2.0 Draft, May 2000, D-18053, Edited by Kelly L. Perry.

This section provides an overview of the QuikSCAT satellite, the main characteristics and principles of the embedded SeaWinds scatterometer and a general explanation of how wind vectors are calculated from scatterometer measurements.

### 2.1. Mission Description

The SeaWinds on QuikSCAT mission is a "quick recovery" mission to fill the gap created by the loss of data from the NASA Scatterometer (NSCAT), when the ADEOS-1 satellite lost power in June 1997. QuikSCAT was launched from California's Vandenberg Air Force Base aboard a Titan II vehicle on June 19, 1999. It will continue to add to the important ocean wind data set begun by NSCAT in September 1996 (ERS-1/2 respectively in 1991 and 1995). A similar version of the SeaWinds instrument will also fly on the Japanese ADEOS-II spacecraft currently scheduled for launch in late-2002.



Figure 1 - The QuikSCAT satellite. Artist view (NASA document)

The SeaWind instrument on the QuikSCAT satellite is a specialized microwave radar (scatterometer) that measures near-surface wind speed and direction under all weather and cloud conditions over Earth's oceans.

Scatterometers use an indirect technique to measure wind velocity over the ocean, since the atmospheric motions themselves do not substantially affect the radiation emitted and received by the radar. These instruments transmit microwave pulses and receive backscattered power from the ocean surface. Changes in wind velocity cause changes in ocean surface roughness, modifying the radar cross-section of the ocean and the magnitude of the backscattered power. Scatterometers measure this backscattered power, allowing estimation of the normalized radar cross section ( $\sigma_0$ ) of the sea surface. Backscatter cross section varies with both wind speed and direction when measured at moderate incidence angles. Multiple, collocated, nearly simultaneous  $\sigma_0$  measurements acquired from several directions can thus be used to solve simultaneously for wind speed and direction.

The first space borne scatterometer flew as part of the Skylab missions in 1973 and 1974, demonstrating that space borne scatterometers were indeed feasible. The SeaSat-A Satellite

Scatterometer (SASS) operated from June to October 1978 and proved that accurate wind velocity measurements could be made from space. The SASS cross section measurements have been used to significantly refine the empirical model relating backscatter to wind velocity, and the SASS data have been applied to a variety of oceanographic and meteorological studies. A single-swath scatterometer operating at C-band is presently flying on the European Space Agency's Earth Remote Sensing (ERS-2) mission, continuing the time series of C-band wind scatterometer measurements, which began on July 7, 1991 with ERS-1. NSCAT was launched on ADEOS-1 (Midori) in August 1996 and returned nearly 10 months of dual-swath, 25-km resolution Ku-band backscatter and wind data until the demise of the spacecraft in June 1997.

## 2.2. Satellite Description

The NASA Quick Scatterometer (QuikSCAT) mission employs a variation of the Ball Commercial Platform 2000 (BCP 2000 "QuikBird") bus and the JPL-supplied scatterometer payload.

The QuikSCAT satellite was launched into a sun-synchronous, 803-kilometre, circular orbit with a local equator crossing time at the ascending node of 6:00 A.M.  $\pm$  30 minutes Nominal Orbital Parameters.

The nominal orbit for QuikSCAT is defined by the following parameters:

**Table 1 - Nominal Orbital Parameters**

Recurrent period	4 days (57 orbits)
Orbital Period	101 minutes (14.25 orbits/day)
Local Sun time at Ascending node	6:00 A.M. $\pm$ 30 minutes
Altitude above Equator	803 km
Inclination	98.616°

## 2.3. SeaWinds Sensor Overview

The SeaWinds instrument uses a rotating dish antenna with two spot beams that sweep in a circular pattern. The antenna radiates microwave pulses at a frequency of 13.4 GHz across broad regions on Earth's surface. The instrument collects data over ocean, land, and ice in a continuous, 1,800-wide-wide band centred on the spacecraft's nadir sub track, making approximately 1.1 million ocean surface wind measurements and covering 90% of Earth's surface each day.

The SeaWinds instrument on QuikSCAT is an active microwave radar designed to measure electromagnetic backscatter from wind roughened ocean surface. QuikSCAT/SeaWinds is a conically scanning pencil-beam scatterometer. A pencil-beam scatterometer has several key advantages over a fan-beam scatterometer; it has a higher signal-to-noise ratio, is smaller in size, and it provides superior coverage.



### 2.3.1. Introduction to QuikSCAT

QuikSCAT has two major systems, the space borne observatory system and the ground data processing system. The SeaWinds observatory instrument is specialised microwave radar designed to measure winds over the oceans

The ground system computers produces wind measurements within 3 days of receiving raw QuikSCAT data from the spacecraft, with no backlog, throughout the mission. QuikSCAT data products currently include global backscatter data and 25 km resolution ocean wind vectors in the measurement swaths. There are also plans to provide spatially and temporally averaged, gridded, wind field maps, and other special products.

### 2.3.2. Principles of Operation

Space borne scatterometers transmit microwave pulses to the ocean surface and measure the backscattered power received at the instrument. Since the atmospheric motions themselves do not substantially affect the radiation emitted and received by the radar, scatterometers use an indirect technique to measure wind velocity over the ocean. Wind stress over the ocean generates ripples and small waves, which roughen the sea surface. These waves modify the radar cross section ( $\sigma_0$ ) of the ocean surface and hence the magnitude of backscattered power

The SeaWinds scatterometer design used for QuikSCAT is a significant departure from the fan-beam scatterometers flown on previous missions (SeaSat SASS and NSCAT). QuikSCAT employs a single 1-meter parabolic antenna dish with twin-offset feeds for vertical and horizontal polarization. The antenna spins at a rate of 18 rpm, scanning two pencil-beam footprint paths at incidence angles of  $46^\circ$  (H-pol.) and  $54^\circ$  (V-pol.)

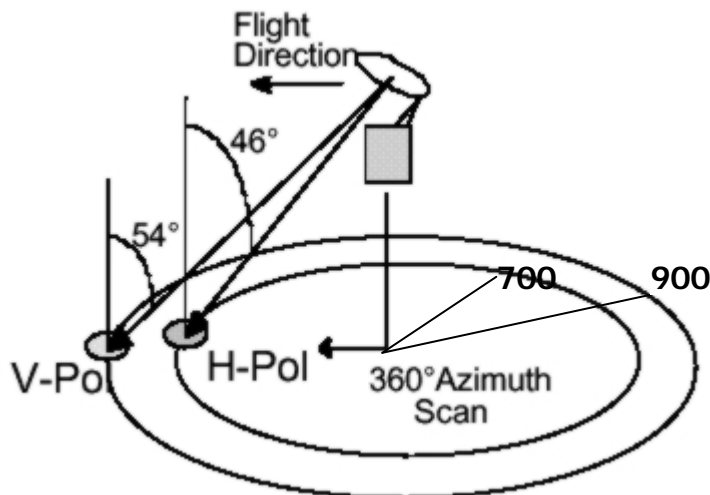


Figure 2 - SeaWinds scanning geometry (adapted from NASA document.)

The transmitted radar pulse is modulated, or “chirped”, and the received pulse (after Doppler compensation) is passed through an FFT stage to provide sub-footprint range resolution. The range resolution is modifiable between 2 km and 10 km, with the nominal value set at about 6 km. The nominal pulse repetition frequency is 187.5 Hz. Each telemetry frame contains data for 100 pulses. Signal and noise measurements are returned in the telemetry for each of the 12 sub-footprint “slices.” Ground processing locates the pulse “egg” and “slice” centroids on the Earth’s surface. The  $\sigma_0$  value is

then computed for both the “egg” and the best 8 of the 12 “slices” (based on location within the antenna gain pattern). The SeaWinds antenna footprint is an ellipse approximately 25-km in azimuth by 37-km in the look (or range) direction. Signal processing provides commendable variable range resolution of approximately 2- to 10-km.

QuikSCAT generates an internal calibration pulse and associated load pulse every half-scan of the antenna. In ground processing, the load pulses are averaged over a 20-minute window, and the cal pulses over a 10-pulse (approximately 18-second) window, to provide current instrument gain calibration needed to convert telemetry data numbers into power measurements for the  $\sigma_0$  calculation. Since the receiver gain is very stable and with careful calibration, the noise power measurements can be converted into apparent brightness temperatures measurements. The observed apparent brightness temperatures are a function of the instrument noise (continuously monitored), the surface emissivity and temperature and the attenuation/emission of the intervening atmosphere (*Jones et al., 2000*). Over the ocean, the brightness temperature measurements are used to locate rain cells and flag the wind vector values, which can be contaminated by rain effects. In the Polar Regions, they are mainly useful in discriminating sea ice covered areas from Open Ocean since the surface emissivity of sea ice is almost twice that of seawater at the operating frequency of QuikSCAT.

## 2.4. Retrieving wind vectors from scatterometer measurements

Scatterometer instruments on board satellites can routinely provide an estimation of the surface wind vector with high spatial and temporal resolution over all ocean basins. Although the exact mechanisms responsible for the measured backscatter power under realistic oceanic conditions are not fully understood, theoretical analysis, controlled laboratory and field experiment, and measurements from space borne radars all confirm that backscatter over the oceans power at moderate incidence angles is substantially dependent on near-surface wind characteristics (speed and direction with respect to the radar viewing geometry). At the present time, the microwave scatterometer is the only satellite sensor that observes wind in terms of wind speed and wind direction.

To date, the most successful inversions of scatterometer measurements rely on empirically derived algorithms. An empirical relationship is typically given by the following harmonic formula:

$$\sigma^0 = \sum_{j=0}^k A_j(\lambda, P, \theta, U) \cos(j\chi) \quad (1)$$

Where  $k$  is the degree of  $\sigma^0$  representation that uses cosines as orthogonal basis (number of harmonics),  $\lambda$ , the scatterometer wavelength,  $P$ , the polarization,  $\theta$ , the radar incidence angle,  $U$  the wind speed for neutral stability and  $\chi$  is the angle between wind direction and radar azimuth.  $A_j(\lambda, P, \theta, U)$  are the model coefficients to be determined through regression analysis.

Surface wind speed and direction at a given height are retrieved through the minimization, in  $U$  and  $\chi$  space, of the Maximum Likelihood Estimator (MLE) function defined by

$$F = - \sum_{i=1}^{i=N} \frac{(\sigma_i^0 - \sigma_{im}^0)^2}{Var(\sigma_{im}^0)} \quad (2)$$

Where  $\sigma^0$  and  $\sigma_{m^0}$  are the measured and estimated, from (1), backscatter coefficients, respectively.  $Var(\sigma_{m^0})$  stands for  $\sigma^0$  variance estimation.  $N$  is the number of measured  $\sigma^0$  used in the wind vector

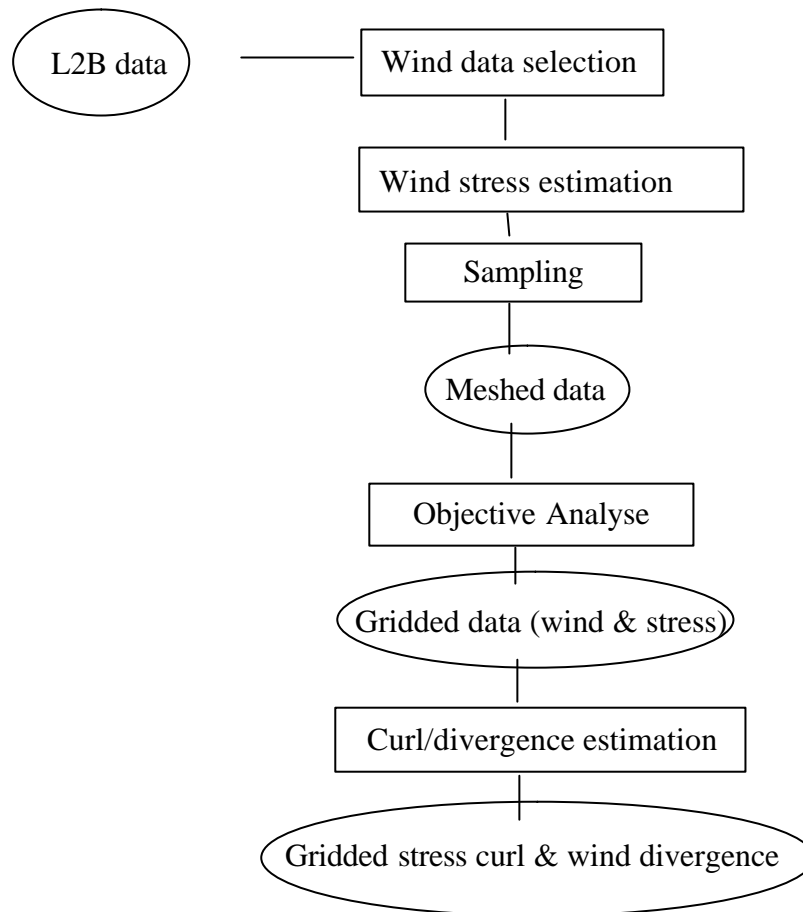
estimation. This approach yields up to four solutions and an ambiguity removal procedure is needed in order to estimate the most probable wind vector (Quilfen *et al*, 1991), (NASA, 1997).

A main task for a scatterometer investigator is the calibration of the sensor data. The calibration involves both the determination of the empirical model (1) and the development of the surface wind retrieval algorithm. A second task consists in validating the accuracy of backscatter coefficients and wind estimates and their comparison with other sources of data.

Since July 1999, two scatterometers are available and provide surface wind estimates with different instrumental configurations. The first one is on board the European Remote Sensing satellite 2 (ERS-2) and the second is the NASA scatterometer SeaWinds on board QuikSCAT. The use of both wind estimates should potentially lead to a more refined wind field analysis calculated from satellite data.

### 3. Processing details

#### 3.1. Processing scheme



#### 3.2. QuikSCAT Level 2B wind data selection

The JPL/PO.DAAC Level 2B product provides wind vectors (wind speed and direction) at 25 km resolution across an 1800 km swath. These scatterometer wind vectors were estimated from the backscatter coefficients using a semi-empirical models and an inversion/ambiguity removal algorithm. The wind vectors used in gridded fields computation are selected from L2B *wind\_speed* (which provide both up to 4 ambiguities), taking the ambiguity indicated in the *wvc\_selection* SDS, and *wind\_dir\_selection* SDS.

Wind vectors whose speed is not in the [0.5 m/s, 30 m/s] range are skipped.

### 3.3. Wind stress estimation

To estimate surface wind stress,  $\tau$ , for each scatterometer wind vector, the bulk formulation is used:

$$\tau = (\tau_x, \tau_y) = \rho C_D W(u, v)$$

Where  $W$ ,  $u$  and  $v$  are the scatterometer wind speed, zonal component (eastward) and meridional component (northward), respectively. The surface wind is assumed to be parallel to the stress vector.  $\rho$  is the density of surface air equal to  $1.225 \text{ kg/m}^3$ .  $C_D$  is the drag coefficient. The magnitude of the stress is:

$$|\tau| = \rho C_D W^2$$

There have been many estimates of  $C_D$ . We have selected the one published and recommended by Smith (1988) which has also been chosen by the WOCE community. The 10 m neutral coefficient formulation over the ocean is

$$C_D = a + b \times W$$

The values of  $a$  and  $b$  are determined for each wind speed range. Figure 5 shows the behaviour of  $C_D$  as a function of wind speed. The main known drag coefficients are also presented.

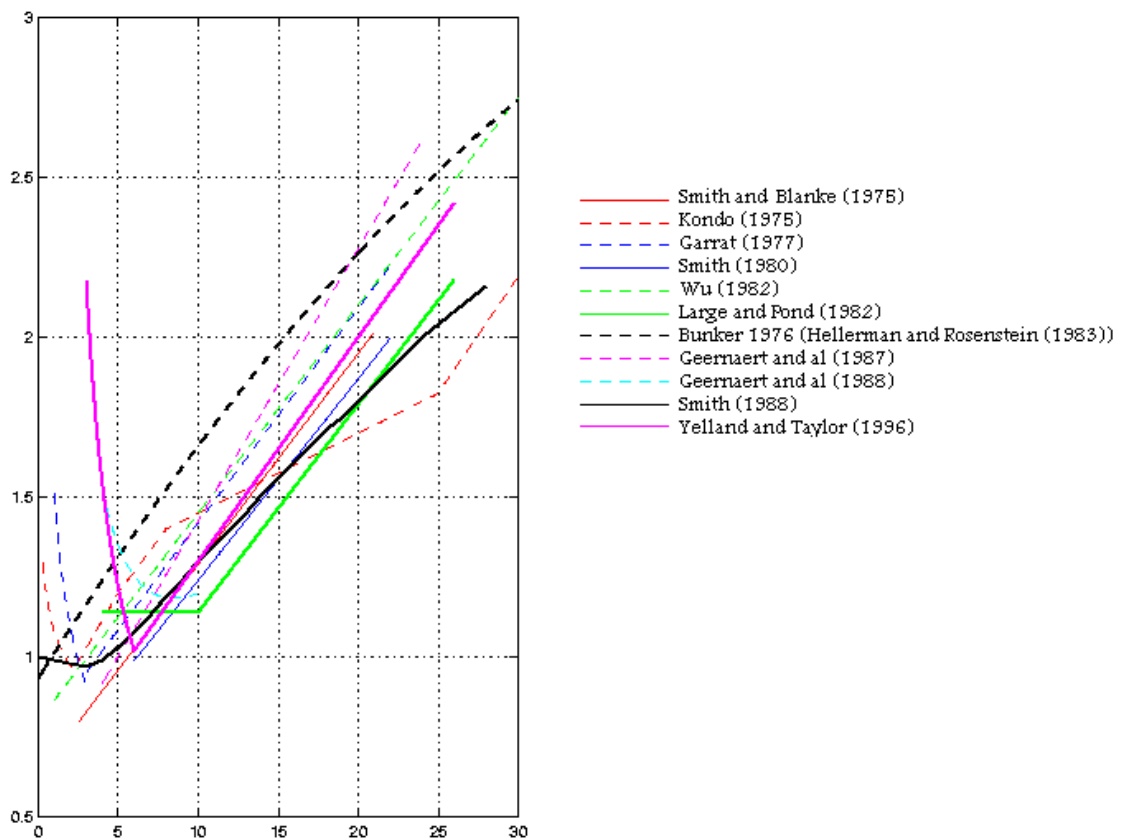


Figure 3 : comparison between various drag coefficients

### 3.4. Sampling

For each scatterometer swath, the data (wind speed, zonal component, meridional component, wind stress, zonal wind stress, and meridional wind stress) are averaged within  $0.5^\circ \times 0.5^\circ$  grid cells in order to reduce spatial dependency between the variables. These averaged measures are thereafter referred as observations. The number of swaths covering each grid cell is recorded.

The sampling distributions of these four  $0.5^\circ \times 0.5^\circ$  scatterometer observations are summarized in Fig. 4. They are evaluated for eight ocean areas indicated by table 2. On average, 5  $0.5^\circ \times 0.5^\circ$  observations are found in each grid point during one day. The distribution of the observation number is quite similar in various regions. In tropical areas, the scatterometer sampling scheme is appropriate to calculate averaged wind fields (Legler, 1991), (Halpern, 1987).

Table 2. : Ocean area coordinates where the scatterometer sampling is evaluated

Zones	Lat. min.,	Long. min.,
	Lat. max.	Long. max.
<b>A/ North Pacific</b>	30, 60	115, 290
<b>B/ North Atlantic</b>	30, 60	290, 20
<b>C/ Indian Ocean</b>	-30, 30	20, 115
<b>D/ Tropical Pacific</b>	-30, 30	115, 290
<b>E/ Tropical Atlantic</b>	-30, 30	290, 20
<b>F/ South Indian Ocean</b>	-60, -30	20, 115
<b>G/ South Pacific</b>	-60, -30	115, 290
<b>H/ South Atlantic</b>	-60, -30	290, 20

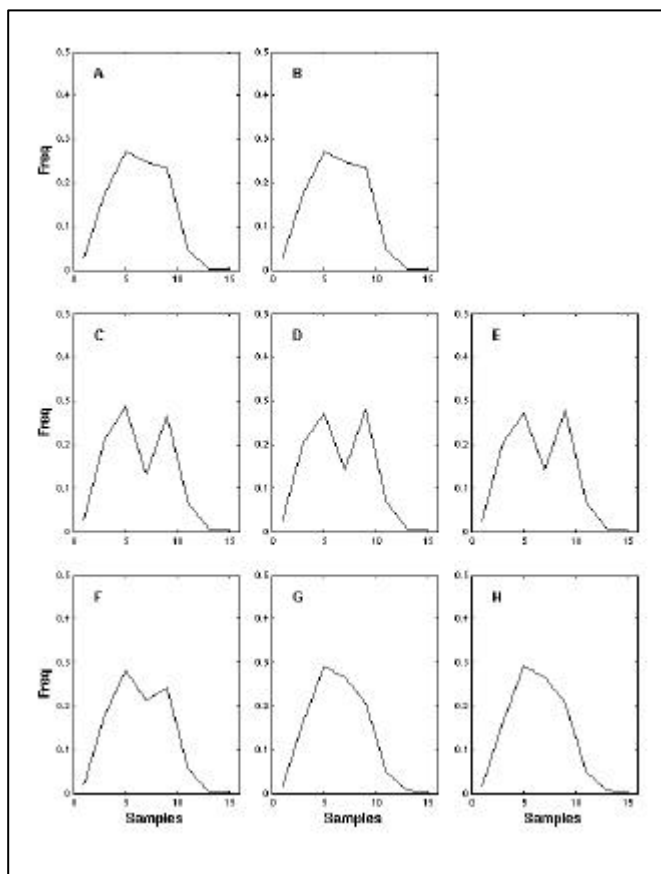
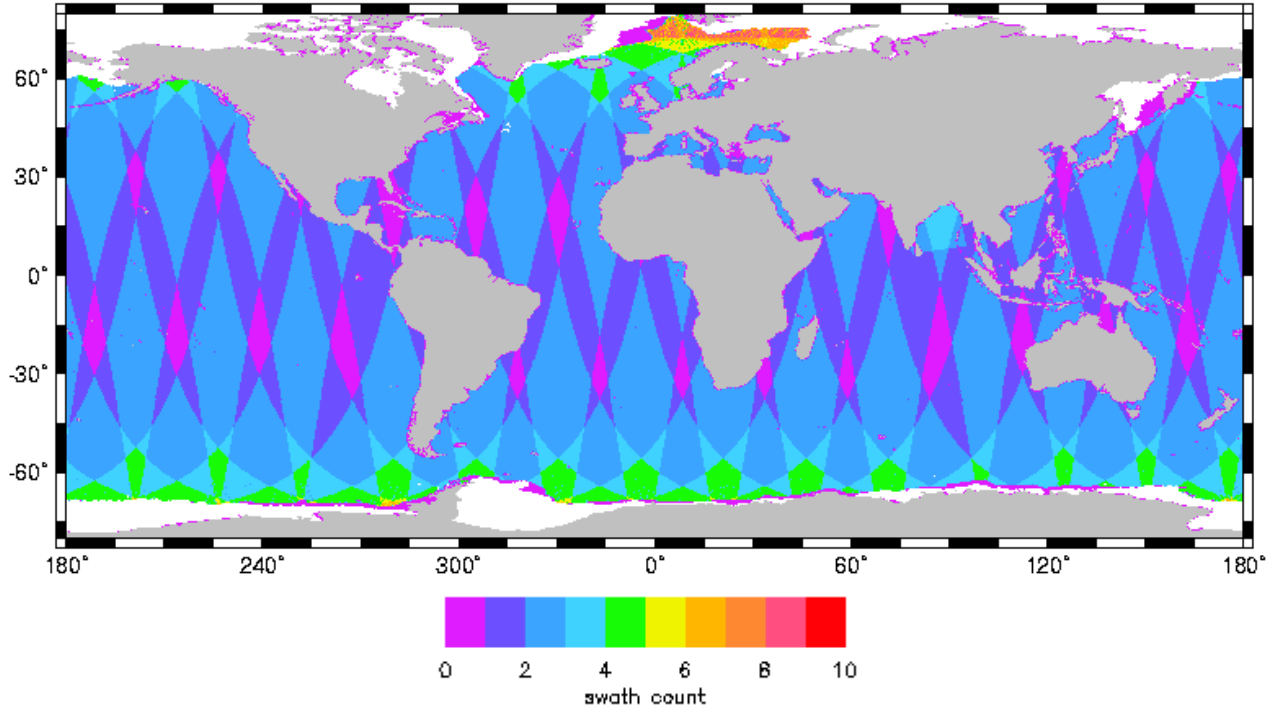


Figure 4

### 3.5. Estimation of gridded wind fields

Since wind estimated at a point can vary significantly over periods of a few hours, it is difficult to reconstruct the synoptic fields of surface winds at basin scales from discrete observations, without the use of an appropriate method. Thus we have developed a statistical technique for the objective analysis of remote sensor wind data. This statistical interpolation is a minimum variance method related to the kriging technique widely used in geophysical studies. The analysis scheme is based on determining the estimator of surface parameters derived from scatterometer measurements. Figure 5 shows an example of seven days of scatterometer coverage.



**Figure 5:** one-day coverage of QuikSCAT scatterometer observations: number of samples in each  $0.5^\circ \times 0.5^\circ$  cell.

The computational details in constructing a regular wind field from polar orbit satellite data are given by Bentamy et al (1996). Briefly, let  $V(X)$  be an observation at point  $X=(x,y,t)$ , where  $x$  and  $y$  are the spatial locations and  $t$  indicates time. We suppose that  $V(X)$  is a realization of the variable  $\langle U \rangle(X)$ .

We assume that each measurement consists of the true value plus a random error:

$$V(X) = \langle U \rangle(X) + \epsilon(X)$$

The analysis scheme is based on the determination of the estimator  $\hat{U}$  of  $\langle U \rangle$ , at a grid point  $X_0$ , of the surface variables using  $N$  observations  $V$  at the point  $X_i$  (referred as **neighbourhood**)

$$U = \sum_{i=1}^N \lambda_i V(X_i), \quad \sum_{i=1}^N \lambda_i = 1$$

Here  $X_i$  stands for spatial and temporal coordinates. The weights  $\lambda$  are determined as the minimum of the linear system named kriging system:

$$-\sum_{i=1}^N \lambda_i \Gamma(i,j) + \Gamma(j,0) - r + \lambda_j \cdot \sigma = 0, \quad \sum_{i=1}^N \lambda_i = 1, j = 1, N$$

Where  $\Gamma$  is the structure function, named variogram. It allows the spatial and temporal variability behaviour of the variable to be estimated. It is defined as:



$$\begin{aligned}
G(i, j) &= C(0, 0) - C(i, j) \\
C(i, j) &= E((\langle U \rangle (X_i) - m)(\langle U \rangle (X_j) - m)) \\
m &= E(\langle U \rangle (X))
\end{aligned}$$

E() and C() indicate the statistical mean and covariance functions, respectively.

Furthermore, the kriging method provides an expression for variance error, named kriging variance, which indicates the accuracy of the estimated wind variable at each grid point. The solution of the kriging system is used to calculate the variance of the difference between the estimated value  $\hat{U}$  and the true value  $\langle U \rangle$  of the surface parameter:

$$E((U - \langle U \rangle)^2) = \Gamma(0,0) + \tau - \sum_{i=1}^N \lambda_i \Gamma(i,0)$$

In order to resolve the kriging system it is necessary to acquire the best possible knowledge of the variogram  $\Gamma$ . Several models exist to define the theoretical formulation of the variogram. In the scatterometer case, the exponential model appears suitable. Its expression in terms of space and time separation is given by the equation:

$$\Gamma(\delta h, \delta t) = \varepsilon + a(1 - \exp(-\frac{(\delta h + \delta t)}{b}))$$

where a, named sill value, corresponds to the variogram value when there is no correlation between variables. b, named spatial variogram range, corresponds to the spatial lag beyond which there is no more structure or where variables are uncorrelated. c is used to indicate the time correlation between variables. Coefficient  $\varepsilon$  corresponds to the spatial noise on scatterometer wind vector estimates. The calculation of  $\varepsilon$  indicates that its value is close to zero.

For instance, table 3.1 gives the estimated values of variogram parameters a, b and c for scatterometer wind speed, zonal component and meridional component in the tropical area.

**Table 3.1 :** Values of the variogram coefficients used for wind speed

	Wind Speed	Zonal Component	Meridional Component
<b>a (m<sup>2</sup>/s<sup>2</sup>)</b>	11.3	49.8	38.1
<b>b(km)</b>	600.	600.	600.
<b>c(km/hour)</b>	30.	30.	30.

**Table 3.2 :** Values of the variogram coefficients used for wind stress

	Wind Stress	Zonal Component	Meridional Component
<b>a (Pa<sup>2</sup>)</b>	0.00335	0.00395	0.00525
<b>b(km)</b>	600.	600.	600.
<b>c(km/hour)</b>	15.85	13.93	23.0

A very sensitive step in this process is, for each grid cell, the determination of a neighbourhood containing the scatterometer data used to estimate the wind vector (wind speeds, zonal and meridional

components). Indeed, due to highly irregular spatial and temporal arrangement and to the density of the scatterometer wind observations, the determination of a local neighbourhood is not straightforward; moreover, a compromise has to be found between an adequate spatial and temporal sampling number and time computing duration.

In the operational method, the neighbourhood is determined taking (for the daily mean fields), every hour (respectively every 6 hours and every 12 hours for weekly and monthly mean fields) in the averaged period, the 4 closest (to the grid cell centre) observations available (if exists) within a 600 km radius depending on the variogram parameters.

### 3.6. Wind divergence and stress curl estimation

The wind divergence,  $Div(V)$ , and the stress curl,  $curl(\tau)$ , at each  $0.5^\circ \times 0.5^\circ$  grid cell are then evaluated from the resultant wind fields. Finite difference schemes are used to estimate the two parameters.

$$Div(V) = \frac{(4/3)[u(i+1, j) - u(i-1, j)] - (1/3)[u(i+2, j) - u(i-2, j)]/2}{2dx} + \frac{(4/3)[v(i, j+1) - v(i, j-1)] - (1/3)[v(i, j+2) - v(i, j-2)]/2}{2dy}$$

$$curl(\tau) = \frac{(4/3)[\tau_y(i+1, j) - \tau_y(i-1, j)] - (1/3)[\tau_y(i+2, j) - \tau_y(i-2, j)]/2}{2dy} - \frac{(4/3)[\tau_x(i, j+1) - \tau_x(i, j-1)] - (1/3)[\tau_x(i, j+2) - \tau_x(i, j-2)]/2}{2dx}$$

where

- $u, v$  are the mean zonal and meridional components of the wind vector (as estimated by kriging),
- $t_x, t_y$  are the mean zonal and meridional components of the wind stress vector (as estimated by kriging),
- $i, j$  are the column and line index of the current grid cell,
- $dx, dy$  are the width and height of the current grid cell

## 4. Product description

This section describes the main characteristics of the QuikSCAT mean wind fields produced at CERSAT, and provides detailed specifications of the format of the data files.

### 4.1. Main characteristics

#### 4.1.1. *Spatial coverage*

The QuikSCAT mean wind fields cover global oceans from 80° North to 80° South in latitude, and 180° West to 180° East in longitude.

#### 4.1.2. *Spatial resolution*

The QuikSCAT mean wind fields are provided on a rectangular 0.5°x0.5° resolution grid.

#### 4.1.3. *Grid description*

The data are projected on a 0.5° rectangular grid of 720 columns and 320 lines. A grid cell spans 0.5° in longitude and 0.5° in latitude. Latitude and longitude of each grid cell refers to its centre. The origin of each data grid is the grid cell defined by 179.75° West in longitude and 79.75° North in latitude. The last grid cell is centered at 79.75° South and 179.75° East.

#### 4.1.4. *Temporal coverage*

Mean winds fields are available from 20 July 1999 to present. They are continually completed.

#### 4.1.5. *Temporal resolution*

Three different temporal resolutions are provided:

- The daily mean covers the time period from 0h to 24h in the current day
- The weekly mean covers the time period from Monday 0h to Sunday 24h in the current week
- The monthly mean covers the time period from the first day at 0h to the last day at 24h in the current month

#### 4.1.6. Land mask

The 0.5° resolution land mask was computed from the GMT coastline database (compiled from World Vector Shorelines -WVS- and CIA World Data Bank -WBDII-). Inner lakes are masked.

#### 4.1.7. Ice mask

No wind values are retrieved over polar sea-ice. The ice mask used is derived from SeaWinds/QRAD open-ocean/sea-ice boundaries computed at CERSAT (refer to the *QuikSCAT Polar Sea Ice Atlas* product, by R.Ezraty – more details on CERSAT web site: <http://www.ifremer/cersat>). The mask edge fits approximately the 40% ice concentration limit.

#### 4.1.8. Main parameters

- Wind speed modulus: 0 – 60 m/s
- Zonal wind component: -60 – 60 m/s
- Meridional wind component: -30 – 30 m/s
- Wind stress modulus: 0 – 2.5 Pa
- Zonal wind stress component: - 2.5 – 2.5 Pa
- Meridional wind stress component: - 2.5 – 2.5 Pa
- Wind vector divergence: -  $10^{-3}$  –  $10^{-3}$  s<sup>-1</sup>
- Wind stress curl: -2.5 – 2.10<sup>-5</sup>
- The estimated error of each at the above parameters is provided with the same unit.

#### 4.1.9. Storage

Data are currently stored as **netCDF** (network Common Data Form) files. Each file contains all parameters for a given date and time resolution (day, week or month) using the following naming convention:

<Start date>-<End date>.nc with dates as 'YYYYMMDDhhmm'

ex: 200010010000-200010020000.nc (daily mean from 1<sup>st</sup> October to 2<sup>nd</sup> October 2000)

200010010000-200011010000.nc (monthly mean, October 2000)

#### 4.1.10. Data volume

About 7 Mo for each file (2 Mo when zipped).

#### 4.1.11. Conventions

Times are UTC.

The longitude reference is the Greenwich meridian: longitude is positive eastward, negative westward and ranges between [-180, 180[ (compatibility within the WOCE package).

The latitude reference is the Equator: latitude is positive in the northern hemisphere, and negative in the southern hemisphere.

## 4.2. Header structure

Element name	Type	Format
WOCE_version	String	3.0
CONVENTIONS	String	"COARDS"
long_name	string	'QuikSCAT <period> mean wind fields' <i>period</i> $\hat{T}$ {daily, weekly, monthly}
short_name	string	'MWF-Q-<period>' <i>period</i> $\hat{T}$ {D,W,M}
producer_agency	string	'IFREMER'
producer_institution	string	'CERSAT'
netcdf_version_id	string	'3.4'
product_version	string	'1.0'
creation_time	string	'YYYY-DDDTHH:MM:SS.SSS'
start_date	string	'YYYY-DDDTHH:MM:SS.SSS'
stop_date	string	'YYYY-DDDTHH:MM:SS.SSS'
time_resolution	string	'<T>' $T\hat{T}$ {one day mean, one week mean, one month mean}
spatial_resolution	string	'0.5 degree'
platform_id	string	'QuikSCAT'
instrument	string	'SeaWinds'
objective_method	string	'kriging'
south_latitude	float	+/-xx.yyyy [-90, 90]
north_latitude	float	+/-xx.yyyy [-90, 90]
west_longitude	float	xxx.yyyy [-180, 180[
east_longitude	float	xxx.yyyy [-180, 180[

### 4.2.1. WOCE\_version

The QuikSCAT mean wind fields are a part of WOCE package. The current WOCE version is "3.0".

### 4.2.2. CONVENTIONS

The netCDF standard conventions to which the product referred. The convention is always "COARDS" that means Cooperative Ocean/Atmosphere Research Data Service. The information on the standard can be found at [http://ferret.wrc.noaa.gov/noaa\\_coop/coop\\_cdf\\_profile.html](http://ferret.wrc.noaa.gov/noaa_coop/coop_cdf_profile.html)

### 4.2.3. long\_name

A complete descriptive name for the product. The long\_name has the format 'QuikSCAT *period* mean wind fields' where *period* is the time interval over which raw data are averaged ('daily', 'weekly', 'monthly').

### 4.2.4. short\_name

The official reference of the product. The format is 'MWF-Q-*period\_id*' where *period\_id* is the identifier of the time interval over which raw data are averaged ('D' for daily means, 'W' for weekly means, 'M' for monthly means).

#### **4.2.5. *producer\_agency***

The agency that provides the project funding. The nominal value is 'IFREMER'.

#### **4.2.6. *producer\_institution***

The institution (here department) that provides project management. The nominal value is 'CERSAT'.

#### **4.2.7. *netcdf\_version\_id***

A character string, which identifies the version of the netcdf (Network Common Data Form) library, which was used to generate this data file. The netcdf libraries are developed by Unidata Program Centre in Boulder, Colorado.

#### **4.2.8. *product\_version***

A character string, which identifies the version of the software, used to generate this data file. The format of this string is *x.y* where *x.y* the release identification number.

#### **4.2.9. *creation\_time***

The clock time when the data file was produced. The format of the date is *YYYY-DDDTHH:MM:SS* where *YYYY* is the calendar year, *DDD* the day of the year, *HH* represents the hour in twenty four hour time, *MM* the minutes and *SS* the seconds.

#### **4.2.10. *start\_date***

The UTC start date of the time interval over which the raw data are averaged on the grid. The format of the date is *YYYY-DDDTHH:MM:SS* where *YYYY* is the calendar year, *DDD* the day of the year, *HH* represents the hour in twenty four hour time, *MM* the minutes and *SS* the seconds.

#### **4.2.11. *stop\_date***

The UTC end date of the time interval over which the raw data are averaged on the grid. The format of the date is *YYYY-DDDTHH:MM:SS* where *YYYY* is the calendar year, *DDD* the day of the year, *HH* represents the hour in twenty four hour time, *MM* the minutes and *SS* the seconds.

#### **4.2.12. *time\_resolution***

The length of the time interval over which the raw data are averaged on the grid. The nominal values are 'one day mean' for the daily means, 'one week mean' for the weekly means and 'one month mean' for the monthly means.

#### **4.2.13. *spatial\_resolution***

The size -in latitude and longitude- of the cells of the product grids. The nominal value is '0.5 degree'.

#### **4.2.14. platform\_id**

The identifier (name) of the satellite on which the wind sensor (scatterometer) is embedded. The nominal value is 'QuikSCAT'.

#### **4.2.15. instrument**

The identifier (name) of the scatterometer collecting the raw wind values averaged on the grids. The nominal value is 'SeaWinds'.

#### **4.2.16. objective\_method**

The objective method used to average the raw wind values and fill the gaps on the grid. The nominal value is 'kriging'.

#### **4.2.17. north\_latitude**

The north latitude of the rectangular grid on which the wind values are averaged. The latitude reference is the Equator : latitude is positive in the northern hemisphere, and negative in the southern hemisphere. The nominal value is 80.00.

#### **4.2.18. south\_latitude**

The south latitude of the rectangular grid on which the wind values are averaged. The latitude reference is the Equator : latitude is positive in the northern hemisphere, and negative in the southern hemisphere. The nominal value is -80.00.

#### **4.2.19. west\_longitude**

The west longitude of the rectangular grid on which the wind values are averaged. The longitude reference is the Greenwich meridian : longitude is positive eastward, negative westward and ranges between [-180, 180[ (compatibility within the WOCE package). The nominal value is -180.00.

#### **4.2.20. east\_longitude**

The east longitude of the rectangular grid on which the wind values are averaged. The longitude reference is the Greenwich meridian : longitude is positive eastward, negative westward and ranges between [-180, 180[ (compatibility within the WOCE package). The nominal value is -180.00.

### **4.3. Data structure**

Element name	conceptual type	storage type	dimensions	units	scale_factor	valid_min	valid_max
time	Integer	Int	[1]	Hours	1		
depth	Real	Float	[1]	m	1	10	10
woce_date	string	int	[1]	UTC			
woce_time	time	float	[1]	UTC			
latitude	real	float	[320]	degrees_north	1	-80	80
longitude	real	float	[720]	degrees_east	1	-180.	179,99
swath_count	integer	short	[320, 720]				
quality_flag	integer	byte	[320, 720]				
wind_speed	real	short	[320, 720]	m/s	0.01	0.	60.
wind_speed_error	real	short	[320, 720]	m/s	0.01	0.	10.
zonal_wind_speed	real	short	[320, 720]	m/s	0.01	-60.	60.
zonal_wind_speed_error	real	short	[320, 720]	m/s	0.01	0.	10.
meridional_wind_speed	real	short	[320, 720]	m/s	0.01	-60.	60.
meridional_wind_speed_error	real	short	[320, 720]	m/s	0.01	0.	10.
wind_speed_divergence	real	short	[320, 720]	s <sup>-1</sup>	10 <sup>-7</sup>	-10 <sup>-3</sup>	10 <sup>-3</sup>
wind_stress	real	short	[320, 720]	Pa	0.001	0.	2.5
wind_stress_error	real	short	[320, 720]	Pa	0.001	0.	1.
zonal_wind_stress	real	short	[320, 720]	Pa	0.001	-2.5	2.5
zonal_wind_stress_error	real	short	[320, 720]	Pa	0.001	0.	1.
meridional_wind_stress	real	short	[320, 720]	Pa	0.001	-2.5	2.5
meridional_wind_stress_error	real	short	[320, 720]	Pa	0.001	0.	1.
wind_stress_curl	real	short	[320, 720]	Pa/m	10 <sup>-9</sup>	-2.10 <sup>-5</sup>	2.10 <sup>-5</sup>



#### 4.3.1. *time*

This parameter indicated the number of hours passed since 1900-1-1 0:0:0. This parameter is included for compatibility within the WOCE package.

Conceptual type	integer
Storage type	Int32
Number of bytes	4
Units	hours
Minimum value	<i>First hour of this file period</i>
Maximum value	<i>Last hour of this file period</i>

#### 4.3.2. *depth*

This parameter indicates the depth of the measurement. QuikSCAT surface wind estimates are calculated at 10m height in neutral condition. Therefore the depth parameter is set to +10 (the sea surface has the depth 0, and the positive depth are above the sea surface). This parameter is included for compatibility within the WOCE package.

Conceptual type	real
Storage type	float
Number of bytes	4
Units	meters
Minimum value	<i>10</i>
Maximum value	<i>10</i>

#### 4.3.3. *woce\_date*

This parameter indicates the date of the averaged period. The value refers to the centre of the time period, in UTC, using the *YYYYMMDD* format. The *start\_date* and *stop\_date* attributes of the *woce\_date* variable indicate the beginning and the end of this period using the same format. The *time\_interval* attribute indicates the time resolution of the averaged period ('one day', 'one week' or 'one month'). This parameter is included for compatibility within the WOCE package and is fully redundant with *start\_date* and *stop\_date* global attributes.

Conceptual type	string
Storage type	Int32
Number of bytes	4
Units	UTC
Start date	<i>YYYYMMDD</i>
Stop date	<i>YYYYMMDD</i>
Time interval	'one'

#### 4.3.4. *woce\_time*

This parameter indicates the time of the averaged period. The value refers to the centre of the time period, in UTC, using the *hhmmss.dd* format. The *start\_time* and *stop\_time* attributes of the *woce\_time* variable indicate the beginning and the end of this period using the same format. This parameter is included for compatibility within the WOCE package and is fully redundant with *start\_date* and *stop\_date* global attributes.

Conceptual type	real
Storage type	float
Number of bytes	4
Units	UTC
Start time	<i>hhmmss.dd</i>
Stop time	<i>hhmmss.dd</i>

#### 4.3.5. *latitude*

This parameter indicates the latitude corresponding to a given grid row. The latitude value refers to the centre of the cells of this row. The latitude reference is the Equator: latitude is positive in the northern hemisphere, and negative in the southern hemisphere.

Conceptual type	real
Storage type	float
Number of bytes	4
Units	degree
Minimum value	-80
Maximum value	80
Scale factor	1.

#### 4.3.6. *longitude*

This parameter indicates the longitude corresponding to a given grid column. The longitude value refers to the centre of the cells of this column. The longitude reference is the Greenwich meridian: longitude is positive eastward, negative westward and ranges between [-180, 180[ (compatibility within the WOCE package).

Conceptual type	real
Storage type	float
Number of bytes	4
Units	degree
Minimum value	-180.00
Maximum value	179.99
Scale factor	1.

#### 4.3.7. *swath\_count*

This parameter indicates the number of averaged scatterometer swaths over a given grid cell.

Conceptual type	integer
Storage type	Int 16
Number of bytes	2
Units	count
Minimum value	0
Maximum value	32767
Scale factor	1

#### 4.3.8. *quality\_flag*

This flag indicates the quality of the mean wind computation over a given grid cell. The significance of each flag value is as follow:

Bit	Definition
0	Ice detection 0 : no ice detected 1 : sea ice detected within the grid cell. No mean wind was computed
1	Land detection 0 : no land detected 1 : land detected within the grid cell. No mean wind was computed
2	Mean wind retrieval 0 : mean wind was correctly retrieved 1 : mean wind was not computed because of too low sampling

3	Mean stress retrieval 0 : mean stress was correctly retrieved 1 : mean stress was not computed because of too low sampling
4	Mean wind in valid range 0 : mean wind was reported in valid range 1 : mean wind was out of valid range
5	Mean stress in valid range 0 : mean stress was reported in valid range 1 : mean stress was out of valid range

Conceptual type	enum
Storage type	int8
Number of bytes	1
Units	n/a
Minimum value	0
Maximum value	255
Scale factor	1

#### **4.3.9. *wind\_speed***

The mean wind speed of the surface wind vector computed within a given grid cell, using the kriging method.

Conceptual type	real
Storage type	int16
Number of bytes	2
Units	m/s
Minimum value	0.0
Maximum value	60.0
Scale factor	0.01

#### **4.3.10. *wind\_speed\_error***

The wind speed error of the surface wind vector computed within a given grid cell, using the kriging method. This parameter indicates the quality of the estimator; for high values, which correspond to sampling problems, low wind speed or high variability, the gridded data should be used carefully.

Conceptual type	real
Storage type	int16
Number of bytes	2
Units	m/s
Minimum value	0
Maximum value	10.0
Scale factor	0.01

#### **4.3.11. *zonal\_wind\_speed***

The mean zonal wind vector component computed within a given grid cell, using the kriging method. The zonal wind component is positive for eastward wind direction.

Conceptual type	real
Storage type	int16
Number of bytes	2
Units	m/s
Minimum value	-60.00

Maximum value	60.00
Scale factor	0.01

#### **4.3.12. zonal\_wind\_speed\_error**

The mean zonal wind vector component error computed within a given grid cell, using the kriging method. This parameter indicates the quality of the estimator; for high values, which correspond to sampling problems, low wind speed or high variability, the gridded data should be used carefully.

Conceptual type	real
Storage type	int16
Number of bytes	2
Units	m/s
Minimum value	0.00
Maximum value	10.00
Scale factor	0.01

#### **4.3.13. meridional\_wind\_speed**

The mean meridional wind vector component computed within a given grid cell, using the kriging method. The meridional wind component is positive for northward wind direction.

Conceptual type	real
Storage type	int16
Number of bytes	2
Units	m/s
Minimum value	-60.00
Maximum value	60.00
Scale factor	0.01

#### **4.3.14. meridional\_wind\_speed\_error**

The mean meridional wind vector component error computed within a given grid cell, using the kriging method. This parameter indicates the quality of the estimator; for high values, which correspond to sampling problems, low wind speed or high variability, the gridded data should be used carefully.

Conceptual type	real
Storage type	int16
Number of bytes	2
Units	m/s
Minimum value	0.00
Maximum value	10.00
Scale factor	0.01

#### **4.3.15. wind\_speed\_divergence**

The divergence of the wind vector, computed from the mean wind vector grids using the second order finite difference scheme.

Conceptual type	real
Storage type	int16
Number of bytes	2
Units	s <sup>-1</sup>

Minimum value	-10 <sup>-3</sup>
Maximum value	10 <sup>-3</sup>
Scale factor	-10 <sup>-7</sup>

#### **4.3.16. *wind\_stress***

The mean surface wind stress magnitude, computed within a given grid cell, uses the kriging method. The wind stress individual measurements used in averaging were calculated from the raw wind values using the Smith (1988) bulk formulation.

Conceptual type	real
Storage type	int16
Number of bytes	2
Units	Pa
Minimum value	0.0
Maximum value	2.5
Scale factor	0.001

#### **4.3.17. *wind\_stress\_error***

The mean error of the surface wind stress magnitude, computed within a given grid cell, using the kriging method. This parameter indicates the quality of the estimator; for high values, which correspond to sampling problems, low wind stress or high variability, the gridded data should be used carefully.

Conceptual type	real
Storage type	int16
Number of bytes	2
Units	Pa
Minimum value	0.0
Maximum value	1.0
Scale factor	0.001

#### **4.3.18. *zonal\_wind\_stress***

The mean zonal surface wind stress component, computed within a given grid cell, uses the kriging method. The wind stress individual measurements used in averaging were calculated from the raw wind values using the Smith (1988) bulk formulation.

Conceptual type	real
Storage type	int16
Number of bytes	2
Units	Pa
Minimum value	-2.5
Maximum value	2.5
Scale factor	0.001

#### **4.3.19. *zonal\_wind\_stress\_error***

The mean error of the zonal surface wind stress component, computed within a given grid cell, using the kriging method. This parameter indicates the quality of the estimator; for high values, which correspond to sampling problems, low wind stress or high variability, the gridded data should be used carefully.

Conceptual type	real
Storage type	int16
Number of bytes	2
Units	Pa
Minimum value	0.0
Maximum value	1.0
Scale factor	0.001

#### **4.3.20. meridional\_wind\_stress**

The mean meridional surface wind stress component, computed within a given grid cell, uses the kriging method. The wind stress individual measurements used in averaging were calculated from the raw wind values using the Smith (1988) bulk formulation.

Conceptual type	real
Storage type	int16
Number of bytes	2
Units	Pa
Minimum value	-2.5
Maximum value	2.5
Scale factor	0.001

#### **4.3.21. meridional\_wind\_stress\_error**

The mean error of the meridional surface wind stress component, computed within a given grid cell, using the kriging method. This parameter indicates the quality of the estimator; for high values, which correspond to sampling problems, low wind stress or high variability, the gridded data should be used carefully.

Conceptual type	real
Storage type	int16
Number of bytes	2
Units	Pa
Minimum value	0.0
Maximum value	1.0
Scale factor	0.001

#### **4.3.22. wind\_stress\_curl**

The curl of the wind stress vector, computed from the mean wind stress vector grids using the second order finite difference scheme.

Conceptual type	real
Storage type	int16
Number of bytes	2
Units	Pa/m
Minimum value	$-2 \cdot 10^{-5}$
Maximum value	$2 \cdot 10^{-5}$
Scale factor	$10^{-9}$

## 5. Data use

### 5.1. Data access

#### 5.1.1. *Ftp access*

All QuikSCAT mean wind fields data files, continually updated, can be downloaded through anonymous ftp at IFREMER/CERSAT: [ftp.ifremer.fr/products/gridded/mwf\\_quiskcat/data](ftp.ifremer.fr/products/gridded/mwf_quiskcat/data)

#### 5.1.2. *WWW access*

All fields can be browsed on CERSAT web site: <http://www.ifremer.fr/cersat>.

Choose 'Data' then 'Extraction'

#### 5.1.3. *On-line browser*

All fields can be browsed on CERSAT web site: <http://www.ifremer.fr/cersat>.

Choose 'Data' then 'Quicklook'

### 5.2. Reading the data

The data produced are stored under the netCDF standard interface for array oriented data access and provides freely distributed libraries for C, Fortran, C++, Java and perl that provide implementation of the interface. Further information can be found at [http://www.unidata.ucar.edu/packages/netcdf/guide.txn\\_doc.html](http://www.unidata.ucar.edu/packages/netcdf/guide.txn_doc.html)

## 6. Validation & accuracy

### 6.1. Accuracy of scatterometer winds

Surface wind is a key parameter in determining of ocean-atmosphere interaction parameters such as latent and sensible air-sea heat fluxes and air-sea carbon dioxide transfer rate, momentum flux and the wind stress on the surface layer of the ocean. Therefore a great deal of effort has been devoted to produce a gridded wind field using scatterometer-retrieved wind vectors over the globe. QuikSCAT description can be found in the *QuikSCAT Mean Wind Field User Manual*, and in the NASA [1]. Briefly, the QuikSCAT scatterometer is in circular orbit with a period of about 101 minutes, at an inclination of  $98.61^\circ$  and at a nominal height of 803 km with a 4-day repeat cycle. QuikSCAT employs a single parabolic antenna with twin-offset feeds for vertical and horizontal polarization. It operates at 13.4 GHz (Ku band) at two incidence angles of  $46^\circ$  (H-pol) and  $52^\circ$  (V-pol). It measures normalized radar cross sections,  $\sigma^0$ . H-pol and V-pol  $\sigma^0$  measurements are performed over 1400 km, and 1800 km wide bands, both centred on the spacecraft nadir sub track. The spatial resolution of the instrument on the earth's surface is about 25 km. The accuracy of the retrieved wind speed and direction was evaluated by comparing with the National Data Buoy Centre (NDBC), Tropical Atmosphere Ocean (TAO) and European buoy wind measurements (**Figure 6**). The scatterometer and buoy data were collocated within 1 hour and 25 km time and space windows. The rms error is less than 1.90 m/s for wind speed and  $17^\circ$  for wind direction, which meet the QuikSCAT wind specifications. However, the mean difference between buoy and satellite wind speeds is about  $-0.35\text{m/s}$ , indicating an overestimation of scatterometer wind speed estimates with respect to buoy measurements. **Figure 7** provides an example of QuikSCAT / buoy wind speed comparisons. It shows scatter plots of the comparison of DIRTH (**Figure 7a and 7c**) and selected (**Figure 7b and 7d**) scatterometer wind speeds with buoy winds at 10-m for the NDC buoys (**Figure 7a and 7b**) and TAO buoys (**Figure 7c and 7d**). The selected winds exhibit more realistic wind speed distribution. The scatterometer winds underestimate at low winds and overestimate at high winds. Concerning the wind direction (**Figure 8**), the Rms difference is about  $16^\circ$ , and meets the goal of QuikSCAT,  $20^\circ$ . As expected, the DIRTH wind directions provide the best correlation with buoy wind estimates.

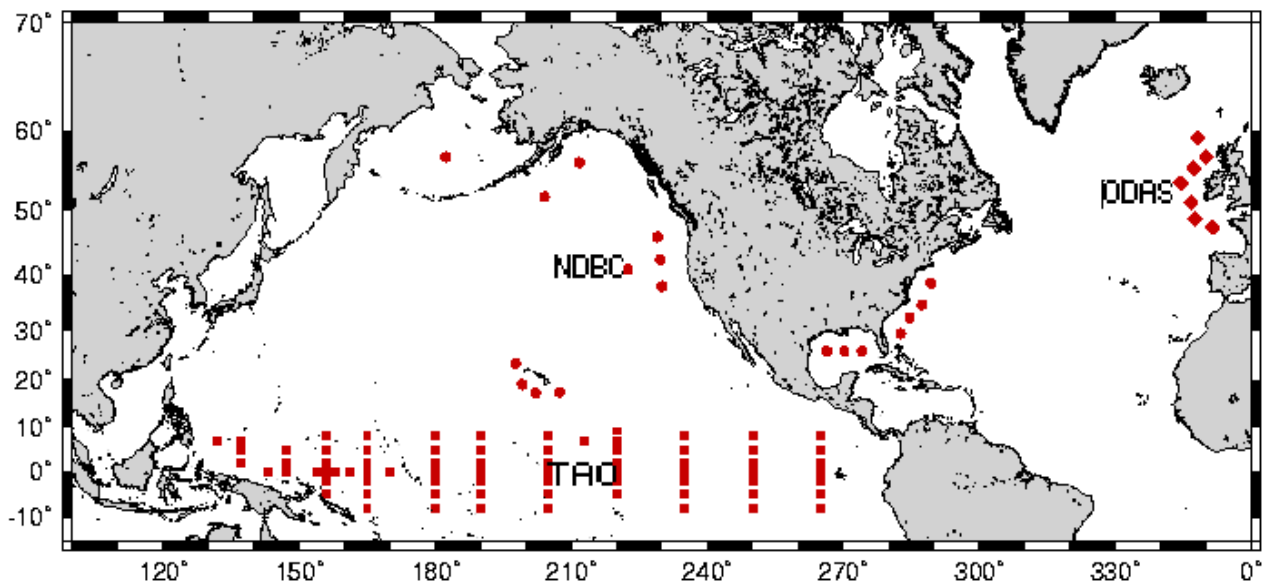


Figure 6



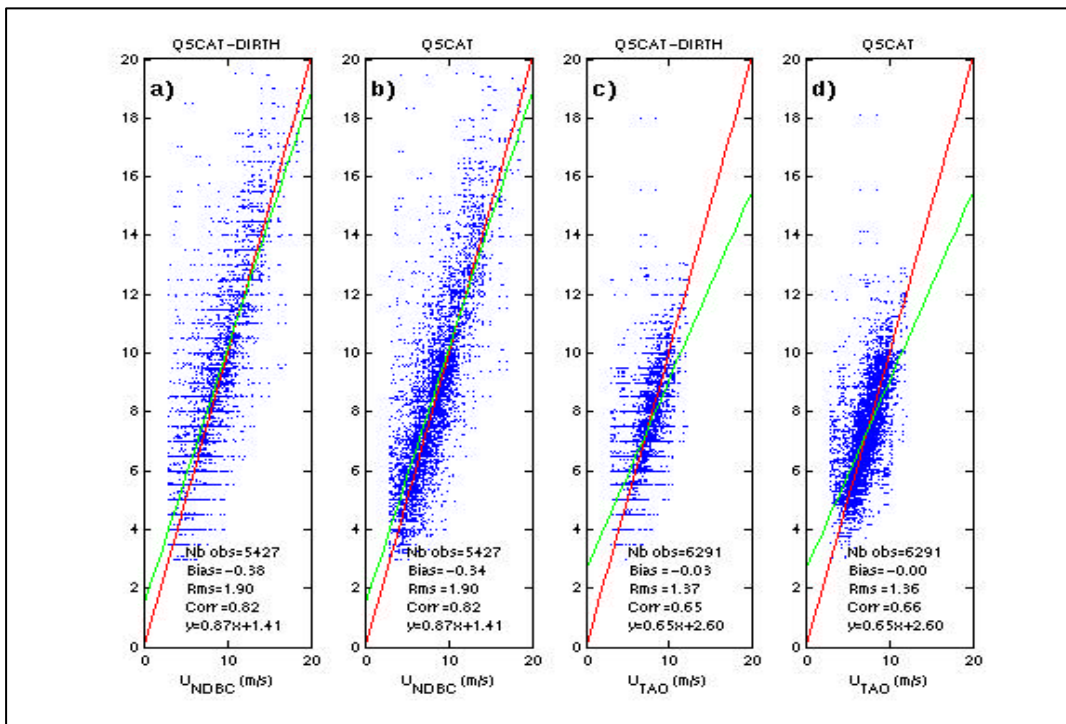


Figure 7

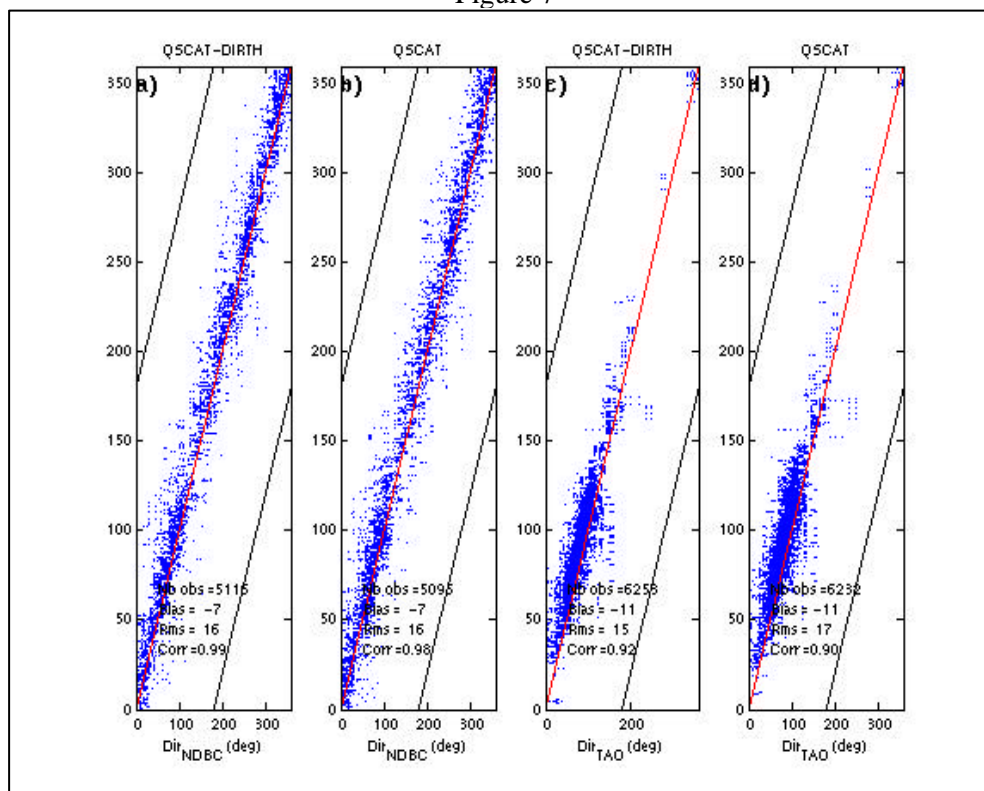


Figure 8

## 6.2. Aliasing in regular wind fields

As indicated in the previous section, the width of a QuikSCAT scatterometer swath is 1800 km. Its orbit is about 110 minutes. Hence, scatterometer wind estimates could be close in space but widely separated in time. In some regions, such as the North Atlantic, wind variability at a given location could be high during a period of a few hours. Even though the kriging method uses a structure function of wind variables, it is necessary to investigate the impact of the number and of

the spatial and temporal distribution of the observations used to estimate wind at each grid point. This involves the impact of scatterometer sampling on the accuracy of the method and also the way the objective method restitutes highly variable events.

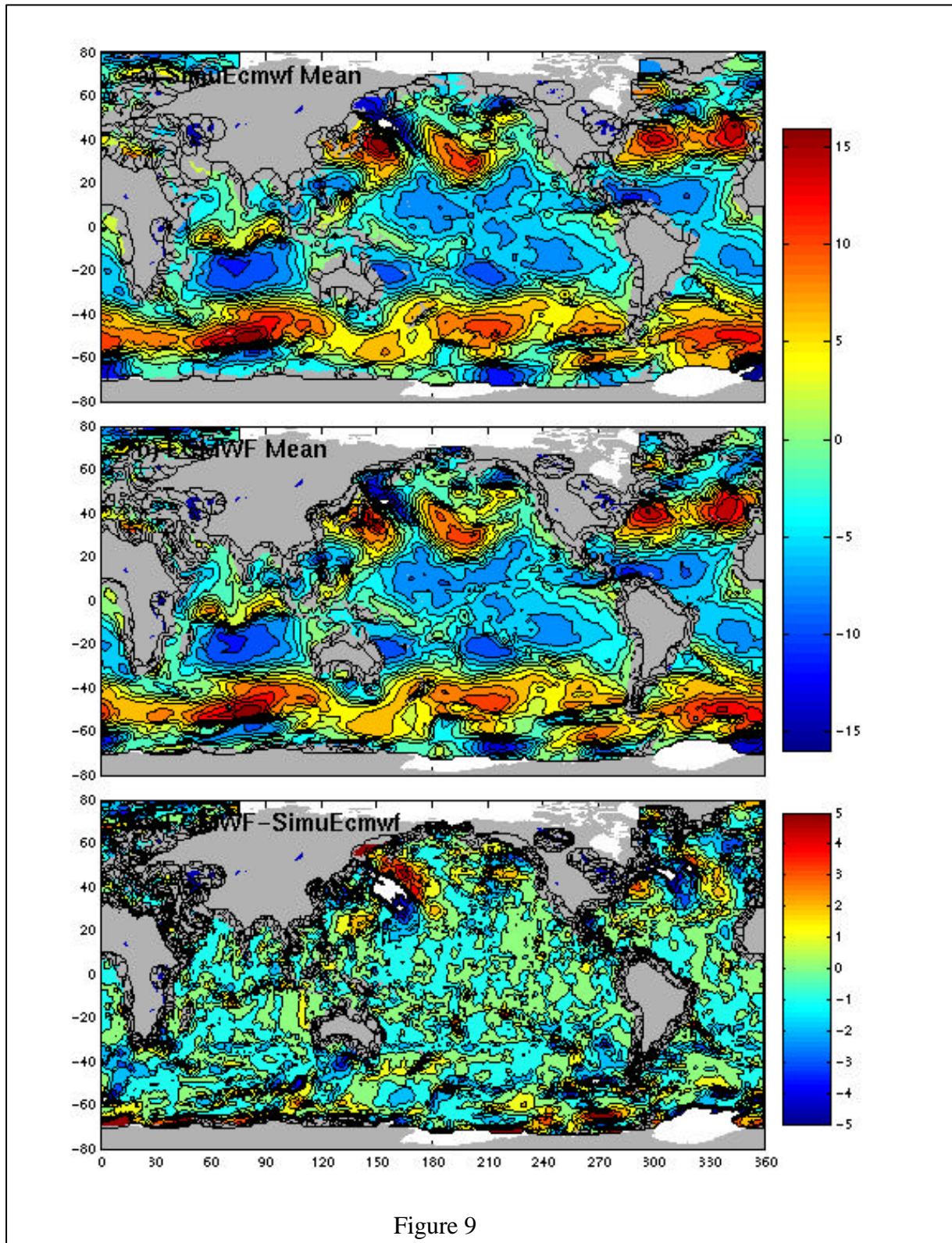


Figure 9

The best way to check the aliasing problem is to simulate scatterometer wind sampling from regular surface wind, considered as the "ground truth", and then to compare the resulting wind field with the initial one. The European Centre for Medium-Range Weather Forecasts (ECMWF) surface wind analysis is used. The spatial resolution of ECMWF analysis is 1.125 x 1.125 deg in longitude and latitude. The analysis is provided at synoptic time (00h, 06h, 12h, 18h). At each scatterometer cell, ECMWF wind data are linearly interpolated in time and space. These simulated scatterometer data,

indicated hereafter by Simu\_Scat, is used to generate a regular wind field using the kriging approach. An example of two weekly wind fields calculated from ECMWF analysis, used as wind field control, and from Simu\_Scat wind data is shown in **Figures 9a** and **9b**, respectively. The averaging period is 1<sup>st</sup> January 2001, when the wind was highly variable in the Northern hemisphere. The comparison between the fields is quite good. They exhibit similar large wind structures. The deviation in Simu\_scat wind speed from the ECMWF analysis is shown in **Figure 9c**. On average the mean and standard deviations in the difference between ECMWF and Simu\_scat are about  $-0.07\text{m/s}$  and  $1.50\text{m/s}$ . Some high difference values are observed. For instance in the north-western part of the Pacific Ocean, the difference exceeds  $3\text{m/s}$ . This is mainly due to scatterometer sampling and to wind variability in this high wind condition region. It is obvious that such wind events cannot be retrieved easily with a limited number of satellite observations falling into each grid point of the area. One result is that the kriging approach does not provide any large banded structures due to polar scatterometer sampling.

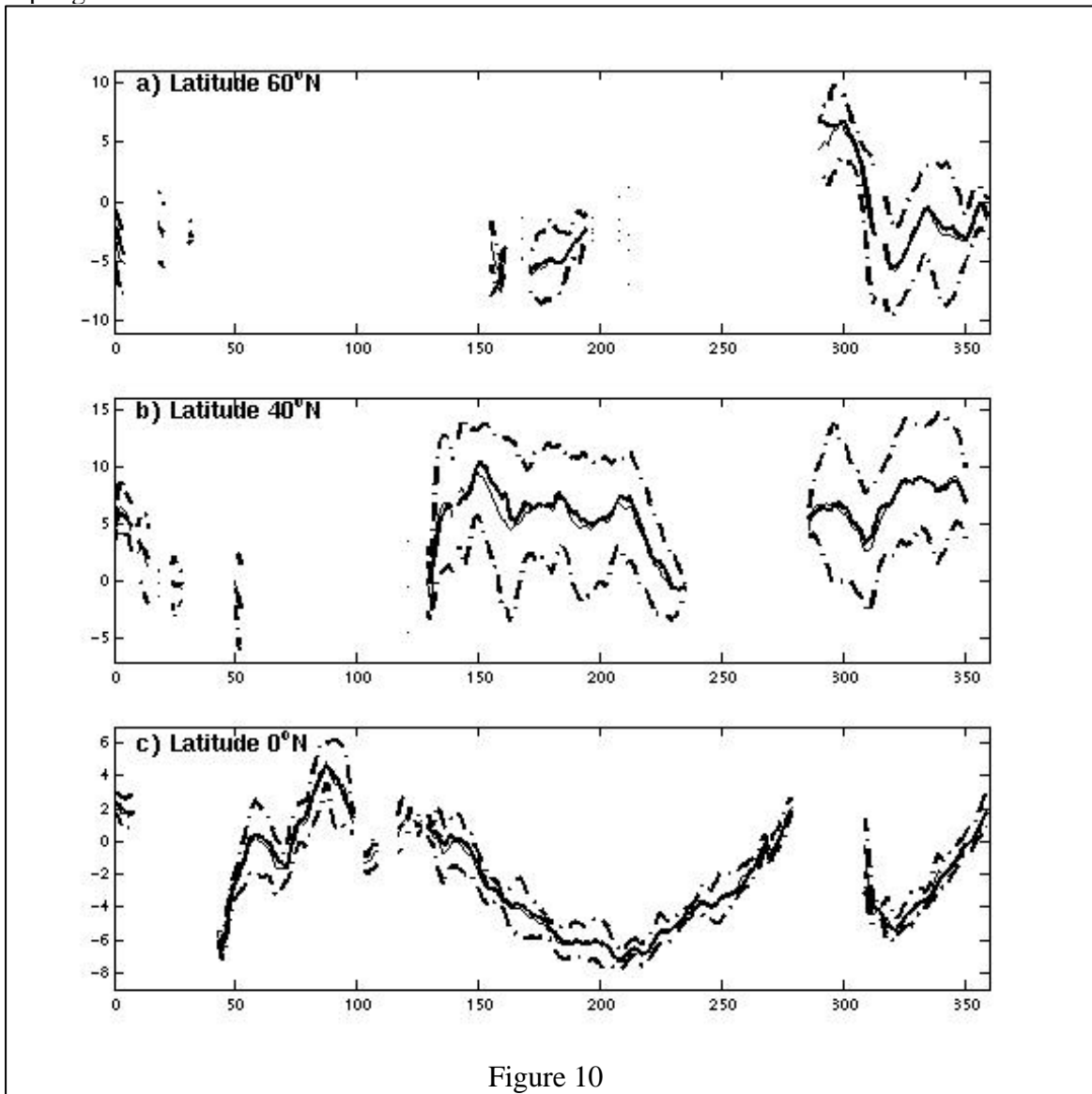


Figure 10

To analyse the impact of the QuikSCAT sampling scheme on the estimation of gridded wind fields, 30 daily wind fields are calculated from ECMWF and Simu\_scat data. The analysis of the scatter plot comparison between true and simulated daily wind fields does not exhibit any systematic errors in the wind estimates (not shown). Generally speaking, the difference between the two fields varies between  $-1.5\text{m/s}$  and  $1.5\text{m/s}$  (in terms of zonal component). However, some high values are found and correspond to the regions where wind variability is high and/or the scatterometer sampling is poor (Bentamy et al, 1998). For instance, let us consider the resulting wind field features at three latitudes in the northern hemisphere:  $60^\circ\text{N}$ ,  $40^\circ\text{N}$ , and equator.

**Figure 10** shows the behaviour of mean zonal component derived ECMWF and Simu\_scatter wind analysis, along these latitudes, according to longitude. It indicates that the agreement between the two estimates is good. The correlation values, estimated at the Equator, between true and simulated variables are about 98%. At 60°N, the correlation drops to 95%. The main discrepancies are observed near coastal areas. **Figure 10** shows that the Simu\_scatter zonal component does not exhibit any systematic 500-1000 km wavelength oscillations.

Similar investigations were performed for weekly and monthly gridded wind fields. As expected the differences are reduced drastically with respect to daily wind field estimates. The highest values of the difference between true and simulated zonal components do not exceed 2 m/s. The percentage of grid points, with respect to the total grid point number, where the difference between ECMWF and simulated scatterometer zonal components exceeds 1.20m/s, accounts for less than 1 %. Most of these high difference values are found in high latitudes.

### 6.3. Comparison of surface winds from QuikSCAT and buoys

The resulting gridded satellite derived winds are compared with averaged buoy observations. Two buoy networks are used in this study (**Figure 6**): The Tropical Atmosphere Ocean (TAO) operated by the Tropical Ocean-Global Atmosphere (TOGA) Program, and the National Data Buoy Centre (NDBC) operated by the National Oceanic and Atmosphere Administration (NOAA). For comparison purposes, the hourly buoy wind speed is converted to a 10-m height in neutral conditions using the *LKB* model. For comparison purposes, the daily averaged buoy data are calculated only if at least 12 hourly estimates are available for each day.

The main statistical parameters characterizing the daily averaged satellite and buoy wind speed ( $W$ ), zonal component ( $U$ ), meridional component ( $V$ ), and wind direction ( $Dir$ ), are listed in Tables 1 and 2, for NDBC and TAO buoy networks, respectively. The daily averaged wind directions are calculated from daily  $U$  and  $V$ . The statistics are calculated for scalar daily wind parameters ( $W_s$  for satellite and  $W_b$  for buoys), and for wind directions  $D_s$  for satellite and  $D_b$  for buoys) as follows:

$$\text{Bias} = \langle W_b - W_s \rangle$$

$$\text{Std (Standard deviation)} = (\langle W_b - W_s \rangle^2 - \text{Bias}^2)^{1/2}$$

$$\text{Corr (Correlation coefficient)} = \frac{\langle (W_b - \overline{W_b})(W_s - \overline{W_s}) \rangle}{\langle (W_b - \overline{W_b})^2 \rangle^{1/2} \langle (W_s - \overline{W_s})^2 \rangle^{1/2}}$$

$$\text{Wind direction difference bias} = \tan^{-1} \left[ \frac{\langle \sin(D_b - D_s) \rangle}{\langle \cos(D_b - D_s) \rangle} \right]$$

$$\text{Wind direction Std} = \sin^{-1}(e) [1 + 0.1547e^3]$$

$$e = \sqrt{1 - [(\sin(D_b - D_s))^2 + (\cos(D_b - D_s))^2]}$$

During the period January – August 2000, there were 5588 and 4869 collocated daily NDBC and QuikSCAT, and TAO and QuikSCAT winds, respectively. The statistics detailed in Table 4 and 2, indicate that the agreement between buoy and satellite winds is good. The RMS differences do not exceed in general 2m/s for wind speed, and 20° for daily wind directions. The correlation coefficients are significantly high. The main discrepancies are found in TAO array, and especially for meridional wind component, and for wind direction. The bias of wind direction difference is about 10°. QuikSCAT winds tend to be clockwise from TAO wind directions. Such results have been found through QuikSCAT and TAO “instantaneous” wind comparisons (**Figure 8**).



The bias on V component is mainly related to wind direction bias. The study of the difference with respect to buoy wind speed ranges indicates that QuikSCAT daily wind speed estimates are slightly overestimated for wind speeds of less than 4m/s. The smallest rms difference is in the 4m/s – 12m/s wind speed range. As for wind direction, the bias is not buoy wind speed dependent, but the standard deviation of the difference is large for wind speeds of less than 4m/s.

## 6.4. Validation of QuikSCAT wind fields over global oceans

In this section, the QuikSCAT gridded wind fields are compared to the operational surface wind analysis estimated at ECMWF. The main aim is to assess the quality of the scatterometer wind estimates on a global scale. The mean daily, weekly and monthly ECMWF wind speed, zonal component and meridional component are obtained from the 6-hourly global analysis datasets on the  $1^{\circ}.125 \times 1^{\circ}.125$  grid. Furthermore, two gridded wind field products, calculated from QuikSCAT wind observations and produced by the Jet Propulsion Laboratory (JPL) group as QuikSCAT level 3 product ([http://podaac.jpl.nasa.gov/pub/ocean\\_wind/quikscat/L3/](http://podaac.jpl.nasa.gov/pub/ocean_wind/quikscat/L3/)), and by *Tang and Liu* (<http://128.149.33.88/seaflex/>), are compared with the daily wind fields generated by the present study. **Figure 11 and 12** show an example of global daily wind fields derived from the four sources. General large scale features of the wind fields are quite similar among IFREMER maps (**Figure 11a, 12a**), QuikSCAT level 3 (**Figure 11b, 12b**), *Tang and Liu* (**Figure 11c, 12c**), and ECMWF (**Figure 11d, 12d**). The lowest wind speeds occur in the equatorial zone, Wind speeds increase pole wards from the equator, with the largest wind speed within latitude bands of  $40^{\circ}\text{S}$ - $60^{\circ}\text{S}$  and  $40^{\circ}\text{N}$ - $60^{\circ}\text{N}$ . However, some discrepancies exist and are mainly related to the method used to calculate gridded wind fields from QuikSCAT wind observations on a global scale.

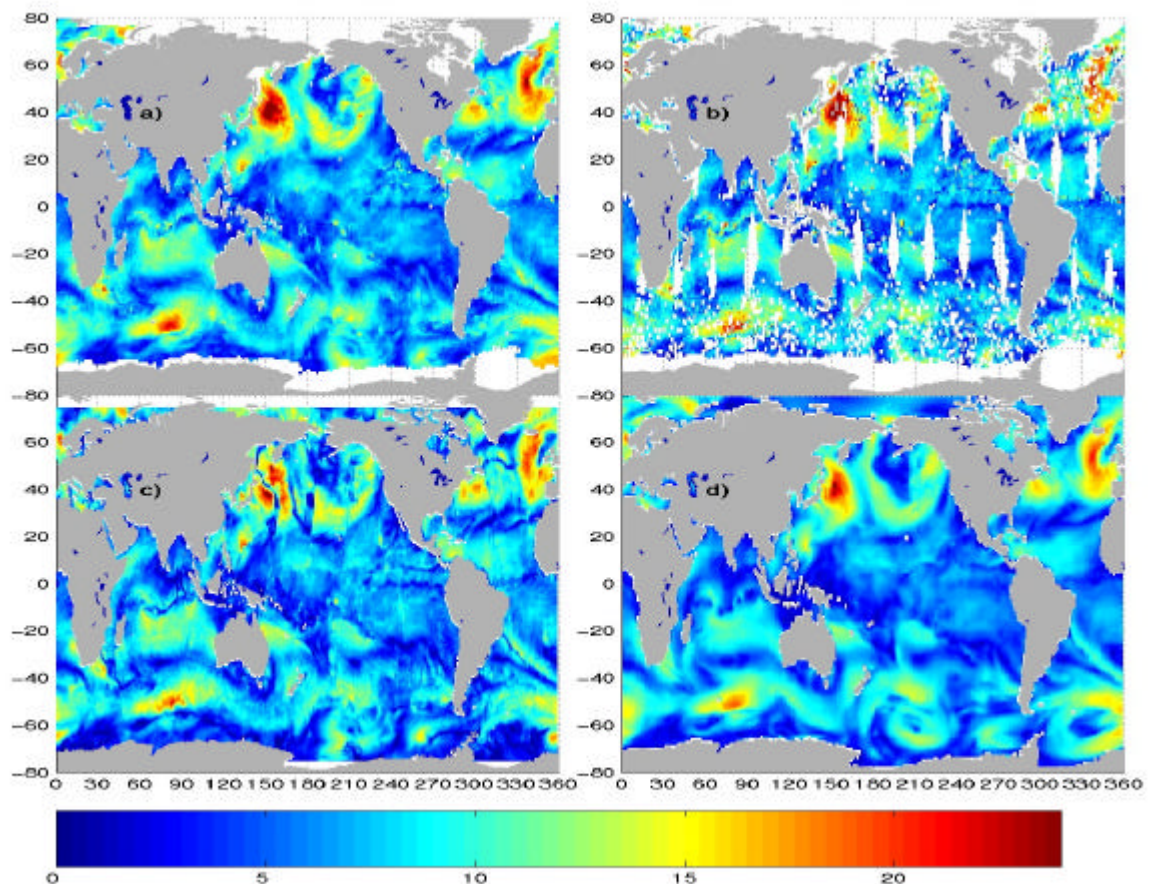


Figure 11

To estimate statistics of differences the four wind fields, thirteen daily wind fields are computed over the global oceans between 60°S and 60°N, from 1<sup>st</sup> through 30<sup>th</sup> January 2001. On average, the daily mean QuikSCAT wind speeds are 0.60 m/s greater than ECMWF wind estimates. This overestimation of QuikSCAT winds with respect to ECMWF is found almost everywhere. For instance, longitudinal and latitudinal averages of the four wind fields are computed in 5°×5° boxes over the global oceans. Figure 8 provides an example of the four daily wind speeds at five boxes centered on 20°W-55°N (**Figure 13a**), 15°W-30°N (**Figure 13b**), 0°E-0°N (**Figure 13c**), 10°E-30°S (**Figure 13d**), and 0°E-55°S (**Figure 13e**). The correlations between various daily wind speeds are high and significant, varying between 0.82 and 0.99. Wind speeds calculated in the present study and derived from QuikSCAT level 3 products are greater than ECMWF at the five locations. At the equator, the difference between ECMWF and QuikSCAT reaches 2m/s.

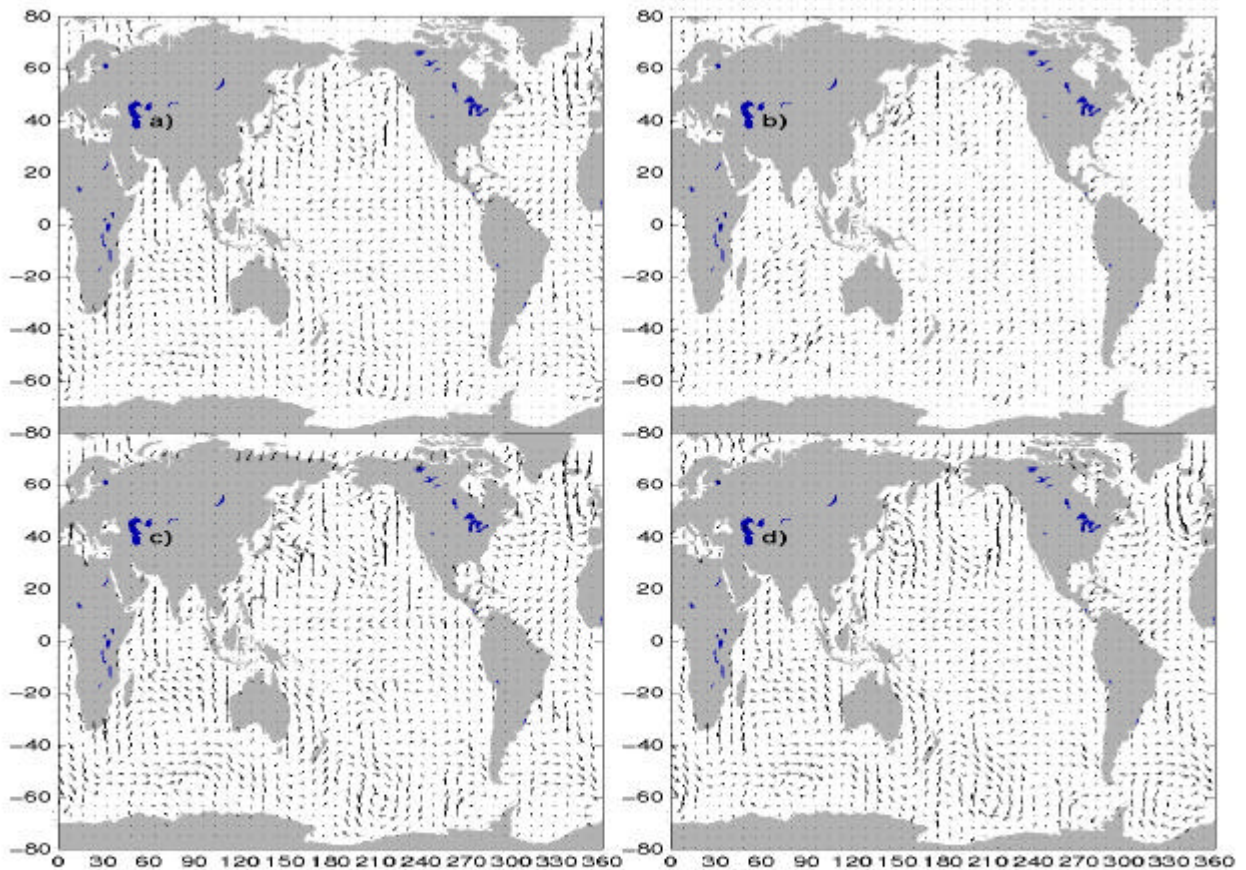


Figure 12

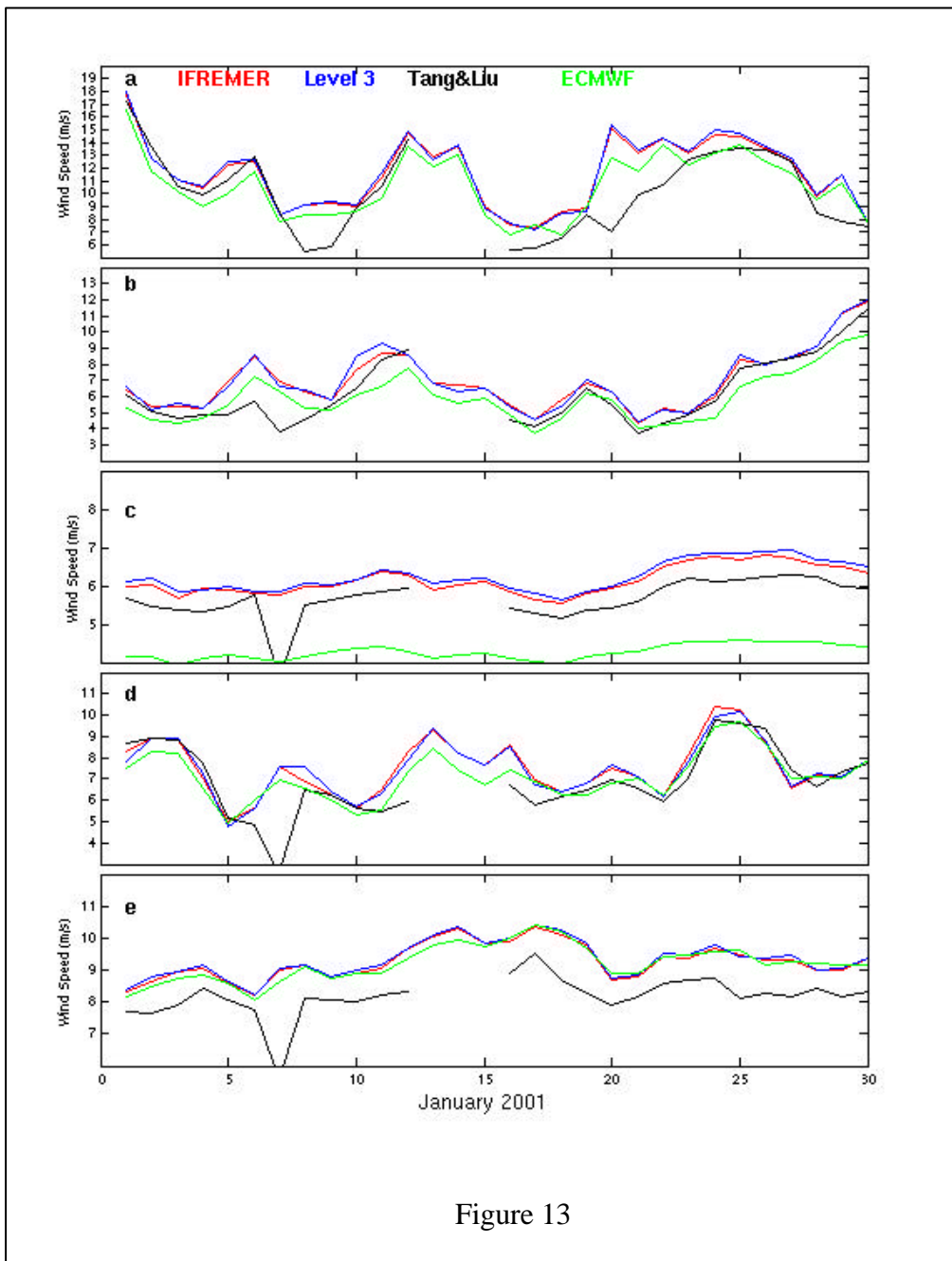


Figure 13

## 6.5. QuikSCAT Mean Wind Field Characteristics

In this section we provide some examples describing the main characteristics of QuikSCAT products in terms of wind field, wind stress, and wind stress curl.

### 6.5.1. Wind Field

The distribution of mean and standard deviation for wind speed, zonal component, and meridional component were calculated over the global oceans from January to December 2000. **Figure 14** shows an example of zonal component distributions. The analysis of such distributions indicated that the main known wind features are present. For instance, the subtropical anticyclonic gyres in the North and South Atlantic, North and South Pacific, and in the Indian Ocean. The lowest and highest winds occur in equatorial and high latitudes (above



50°N and 50°S), respectively. In the Atlantic and Pacific Oceans, surface wind is mainly westwards, corresponding to the trade wind areas (**Figure 14a**). Later in the Indian Ocean, the wind is mainly westwards in the northern part, while in the southern part it is eastwards. The highest zonal components exceeding 8m/s are found between 10°N and 25°N. The maximum in the westerly regions reaches 4.5m/s in the northern latitudes (40°N – 55°N), and 12m/s in the southern latitudes (50°S – 60°S). The largest values of zonal component standard deviation (**Figure 14b**) are found in extra tropical areas. In the northwesterly regions, the standard deviation exceeds 6m/s. This is mainly related to the fact that the wind direction changes with several time scales including seasonal and inter-seasonal ones. Some high values are also found in the northern part of the Indian Ocean corresponding to monsoon variability. In equatorial regions, the highest values of standard deviation are located in the eastern part of the Pacific Ocean, reflecting the Inter-Tropical Convergence Zone (ITCZ) variability.

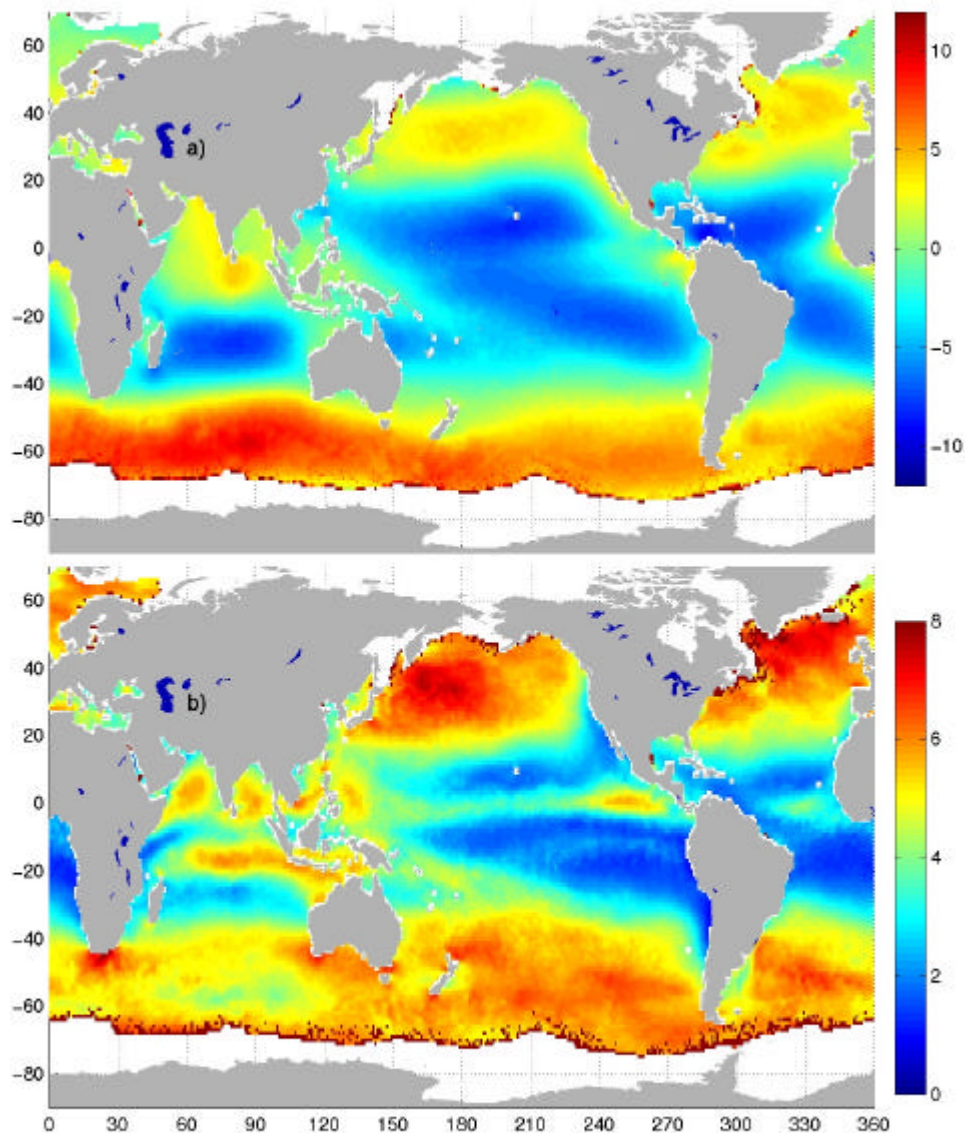


Figure 14



## 6.5.2. Wind Stress

The surface wind stress estimates are evaluated over each QuikSCAT Wind Vector Cell (WVC) from validated wind speed ( $W$ ), zonal component ( $U$ ), and meridional component ( $V$ ) using the following bulk aerodynamic formulae:

$$\mathbf{t} = (t_x, t_y) = \rho C_{D10N} (U, V)$$

$\rho$  is the density of air.  $C_{D10N}$  is the drag coefficient depending on wind speed and considered in neutral conditions [3]. As for wind fields, daily, weekly, and monthly wind stress magnitude ( $t$ ), wind stress zonal component ( $t_x$ ), and wind stress meridional component ( $t_y$ ) are computed.

Figure 10 provides an example of daily wind stress zonal component calculated from QuikSCAT wind observations for 3<sup>rd</sup> January 2000 (**Figure 15a**). The resulting wind stress field is compared to wind stress calculated from ECMWF wind estimates using the Smith algorithm (Smith *et al*, 1988) (**Figure 15b**) or Beljaars model [4] (**Figure 15c**), and to wind stress calculated through a method using SSM/I data ([http://daac.gsfc.nasa.gov/CAMPAIGN\\_DOCS/hydrology](http://daac.gsfc.nasa.gov/CAMPAIGN_DOCS/hydrology)). (**Figure 15d**). The four wind stress fields exhibit similar large scale features. The main differences are related to smoothness and small scale wind features.

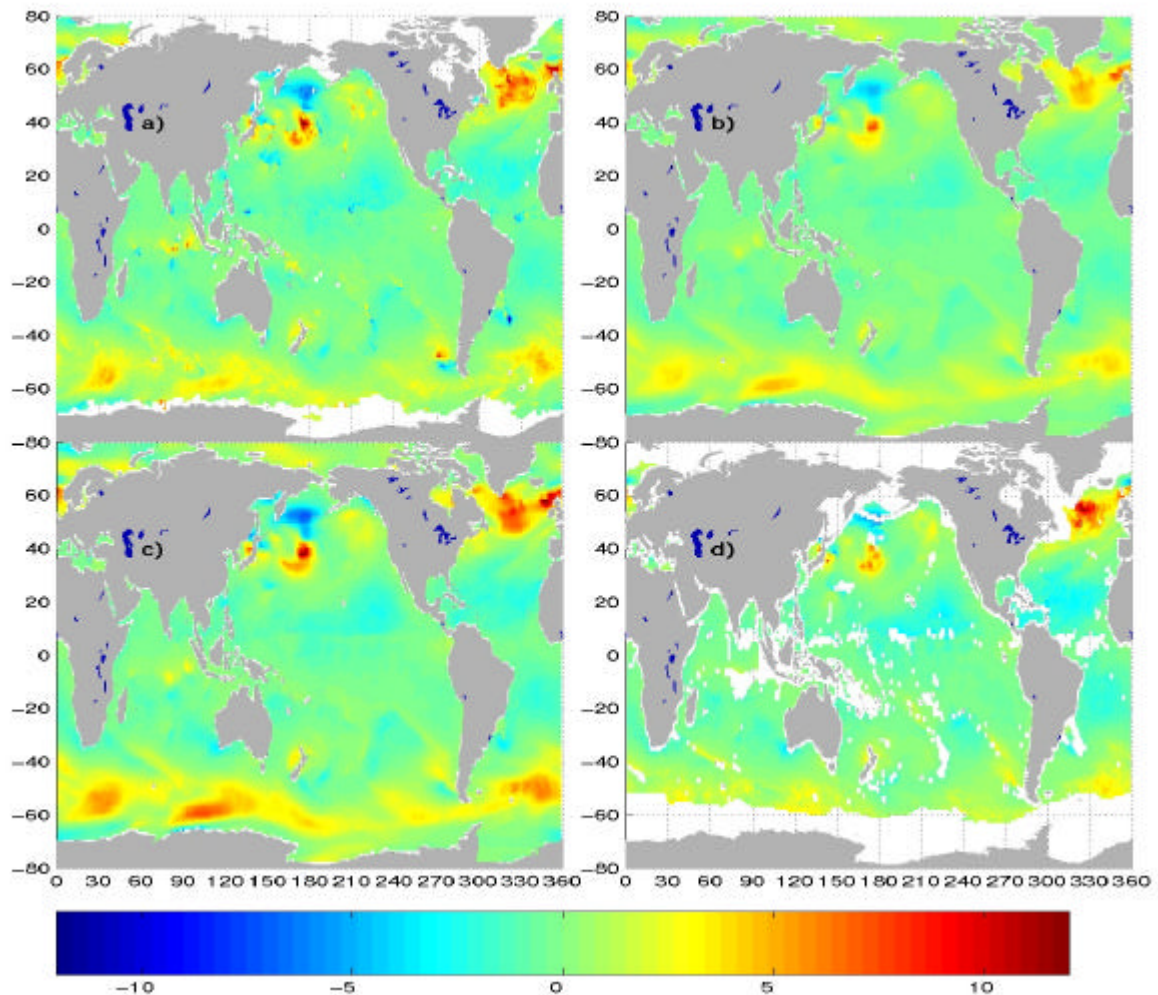


Figure 15

As for the wind vector field, the global distribution of the annual mean and standard deviation wind stress (magnitude, zonal and meridional components) is calculated. An example in terms of wind stress direction and magnitude is shown in Figure 11. Generally speaking, the present results reproduce the wind vector distribution shown in the previous section. They are in good agreement with the main published wind stress climatologies. As expected, wind stress values exceeding  $2 \text{ dyn cm}^{-2}$  are located in the high latitudes of both hemispheres. In intertropical areas ( $30^\circ\text{S} - 30^\circ\text{N}$ ), wind stress values are mostly between  $0.5 \cdot 10^{-1} \text{ N/m}^2$  and  $1.5 \cdot 10^{-1} \text{ N/m}^2$ . However, the annual mean wind stress is much larger in the Southern Hemisphere than in the Northern Hemisphere, exceeding  $2 \cdot 10^{-1} \text{ N/m}^2$  almost over  $360^\circ$  longitude. The maximum westward wind stress exceeding  $1.5 \cdot 10^{-1} \text{ N/m}^2$  is found in the southern part of the Indian Ocean. A strong equator wards wind stress is depicted to the west of most continents, favorable to upwelling events. The **Figure 16** example also shows some interesting small scale features like the Hawaiian Islands ( $160^\circ\text{W}$ ,  $20^\circ\text{N}$ ), and in the Atlantic Ocean near location  $30^\circ\text{W}$ ,  $20^\circ\text{N}$ . Such features, which are also apparent in previous climatologies such as the ERS wind atlas (<http://www.ifremer.fr/cersat>), are due to changes in both wind speed and direction.

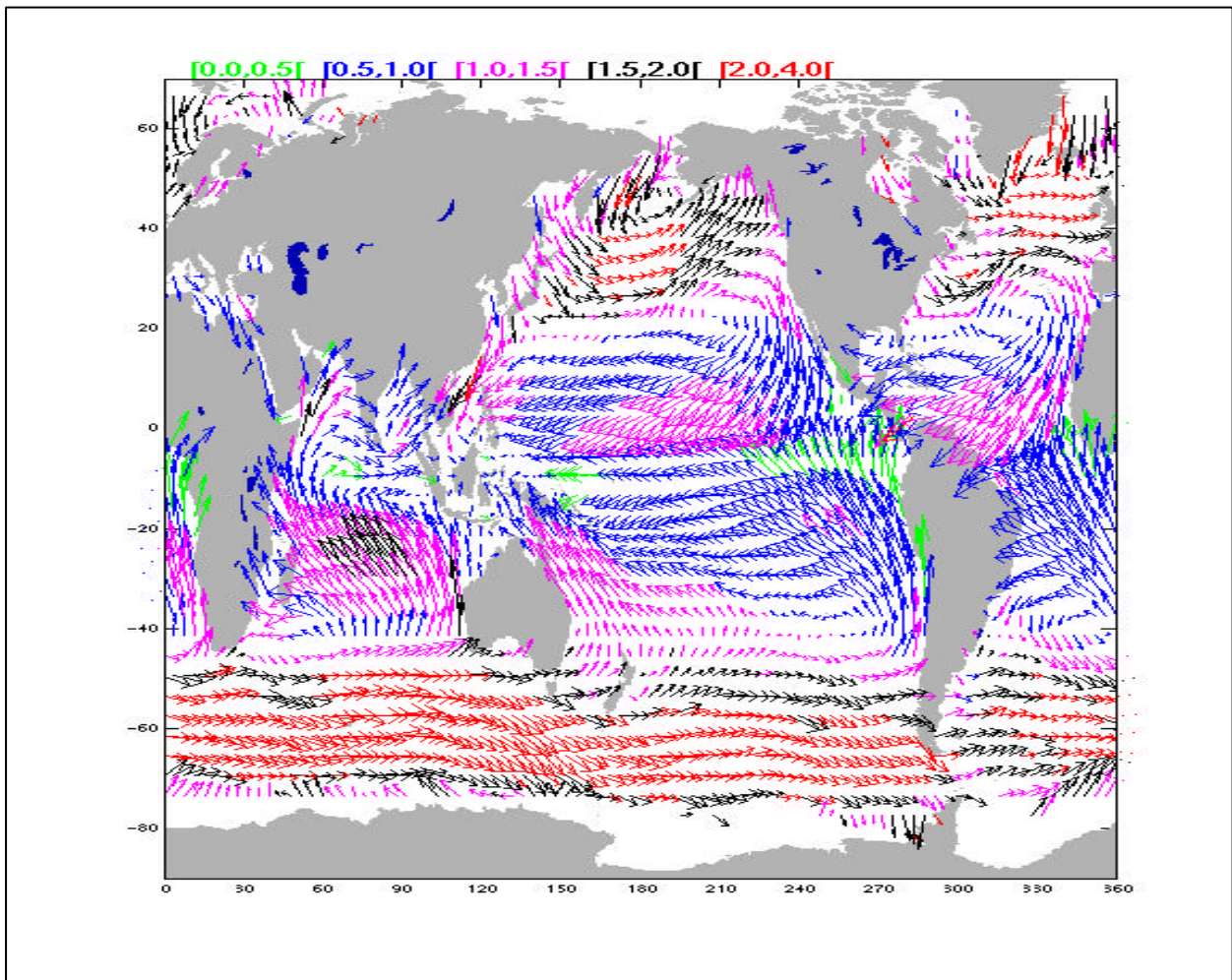


Figure 16

Longitudinal averages of the gridded QuikSCat wind stress are computed in  $2^\circ$  latitude bins for the four seasons winter (December-January-February), spring (March-April-May), summer (June-July-August), and fall (September-October-November) of the year 2000 (**Figure 17**). They reveal the seasonality of atmospheric circulation primarily in high latitude regions of the North Atlantic and Pacific Oceans. This is related to a strong cyclonic circulation during the NH Winter, and to the anticyclonic circulation in the northern summer. For instance, there is a factor of 3 between northern winter and summer wind stress for latitudes higher than  $30^\circ\text{N}$ . The Indian monsoon is also apparent during the northern summer with a stress magnitude of  $1.8 \cdot 10^{-1} \text{ N/m}^2$  at  $10^\circ\text{N}$ . Over southern oceans ( $40^\circ\text{S} - 60^\circ\text{S}$ ), wind stress is quite high during the four

seasons. Therefore, the seasonal changes appear small. The standard deviations (**Figure 17a, b, and c**) from the mean wind stress values show significant longitudinal variations at those latitudes where the wind stress magnitudes are correspondingly large. We note that the mean values and variability of wind stress, calculated at the equator in the Pacific and Atlantic Oceans, are comparable.

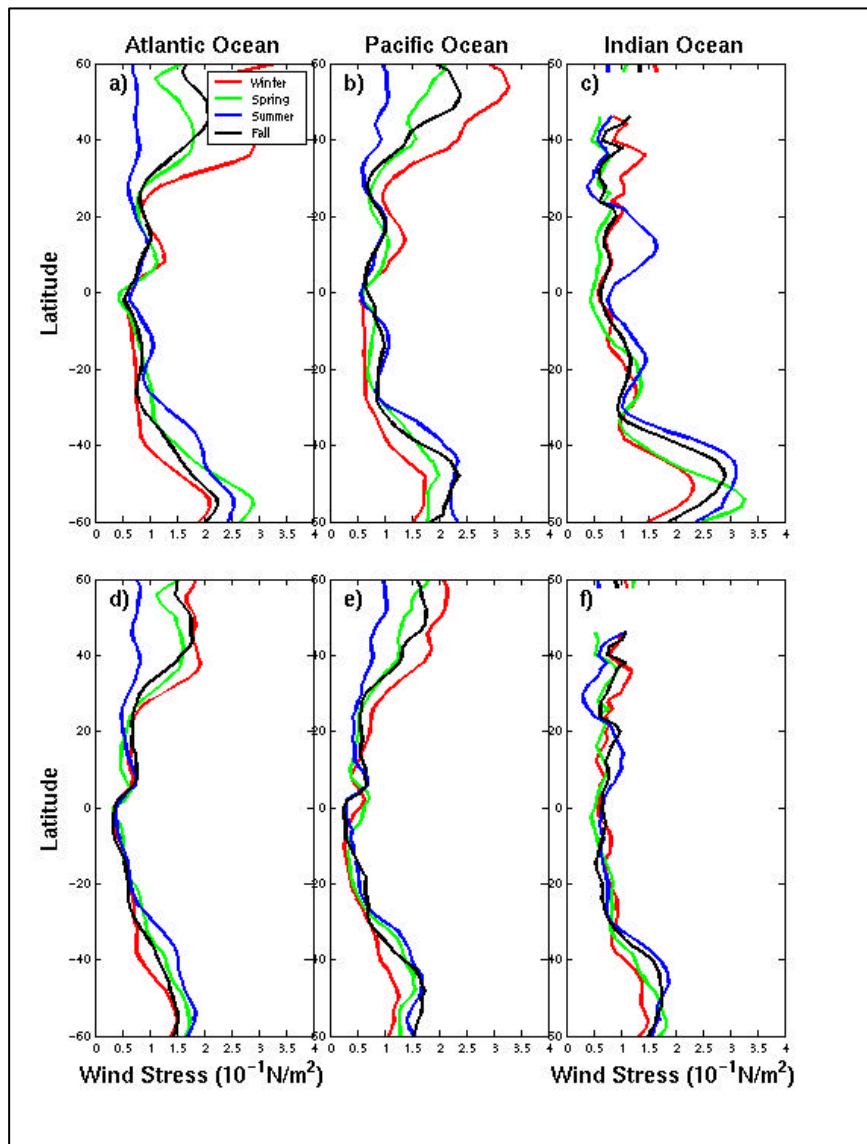


Figure 17

### 6.5.3. Wind Divergence and Wind Stress Curl

The wind vector divergence and wind stress curl for each grid point ( $0.5^\circ \times 0.5^\circ$ ) are calculated from the gridded wind vector and wind stress components in nine surrounding grids by the centre finite difference.

**Figure 18** shows an example of the annual mean wind vector divergence field calculated from QuikSCAT gridded wind components. The main characteristics of such wind parameters are clearly revealed: the intertropical convergence zones in the equatorial areas of the eastern Atlantic and Pacific Oceans, narrow meridional and long zonal convergence in the equatorial Pacific and Atlantic basins, the large divergence values are found near the eastern coasts of most continents.



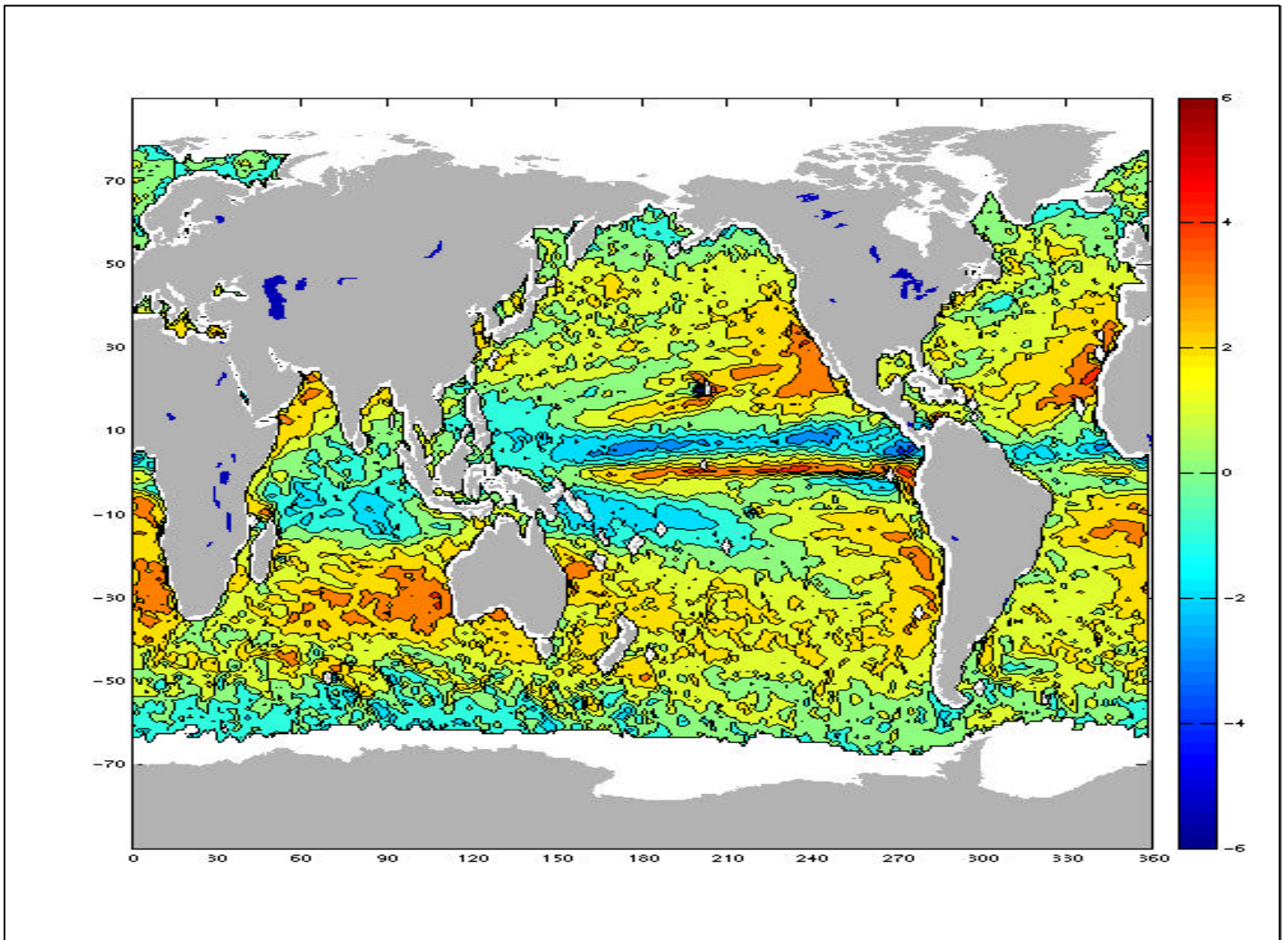


Figure 18

The annual mean wind stress curl over the global oceans and calculated over the year 2000, is shown in **Figure 19**. The main known wind stress curl features are clearly depicted. The east-west slope of the boundary between positive and negative values is evident in the north Atlantic and Pacific Oceans. In the latter basins, the zero wind stress curl lines delineate the northward and southward transport of the sub polar and subtropical gyres, respectively. In the Indian Ocean, the wind stress curl is mostly negative. In the Atlantic and Pacific equatorial basins, the wind stress curl presents narrow zonal bands. The mean annual QuikSCAT wind stress curl values are in agreement with the earlier estimations performed from ERS or NSCAT wind observations [5]. The present curl fields, however, reveal more detailed and fine structures. For instance, near the Hawaii Islands, wind stress curl exhibits a dipole structure with a high positive region in the north, and a negative region in the south. Several other maxima are shown in **Figure 19**. Most of such features are related to narrow cross-shore flows and /or to topography.

The quality of the QuikSCAT wind stress curl may be evaluated through the Sverdrup transports ( $\psi_s$ ), which can be used to assess the oceanic response to atmospheric forcing. **Figure 20** shows the annual mean (January - December 2000) of  $\psi_s$  between 30°S and 45°N, assuming that a steady state was reached for mean annual forcing. In the regions located north 15°N and south 20°S, the  $\psi_s$  values are positive and negative, respectively. For instance, in the NH  $\psi_s$  features correspond to the anticyclonic subtropical gyre including the Kuroshio (Pacific) and Gulf Stream (Atlantic) as the return flow boundary currents. The maximum annual mean circulation is 55 Sverdrups (1Sverdrup (Sv)  $\equiv 10^6$  m<sup>3</sup>/s.) found in the Pacific western boundary area (~ 30°N) In the northwestern part of the Atlantic Ocean, the maximum value is 30Sv.

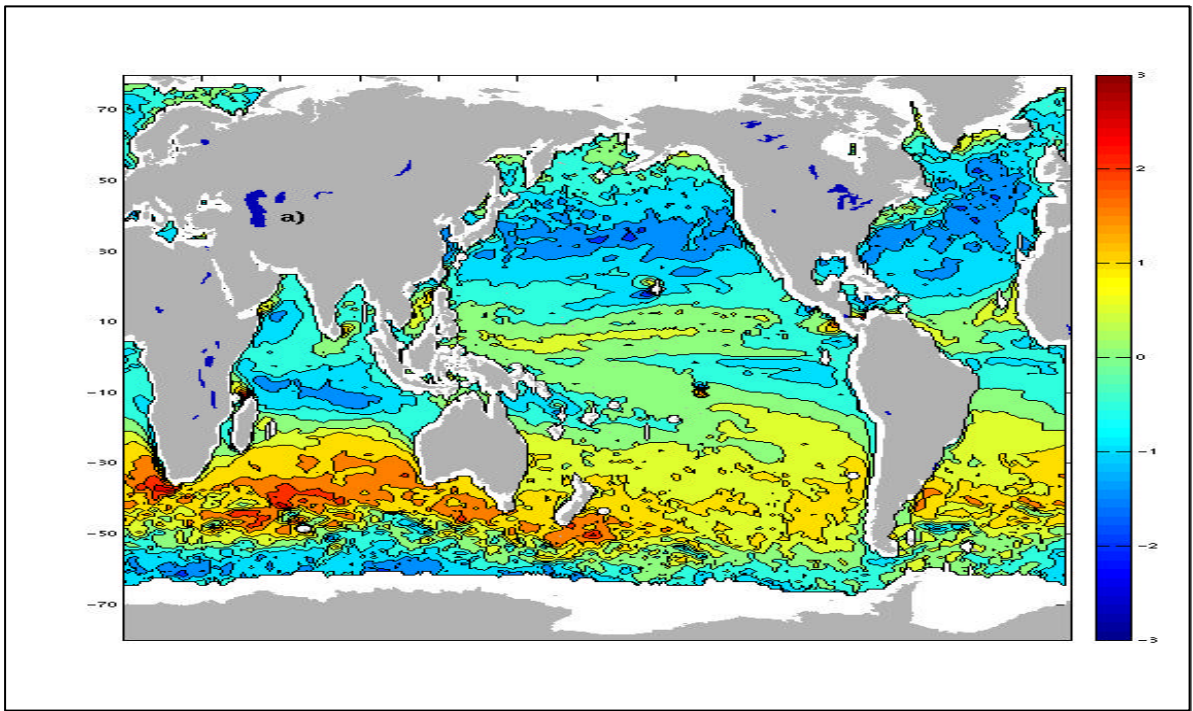


Figure 19

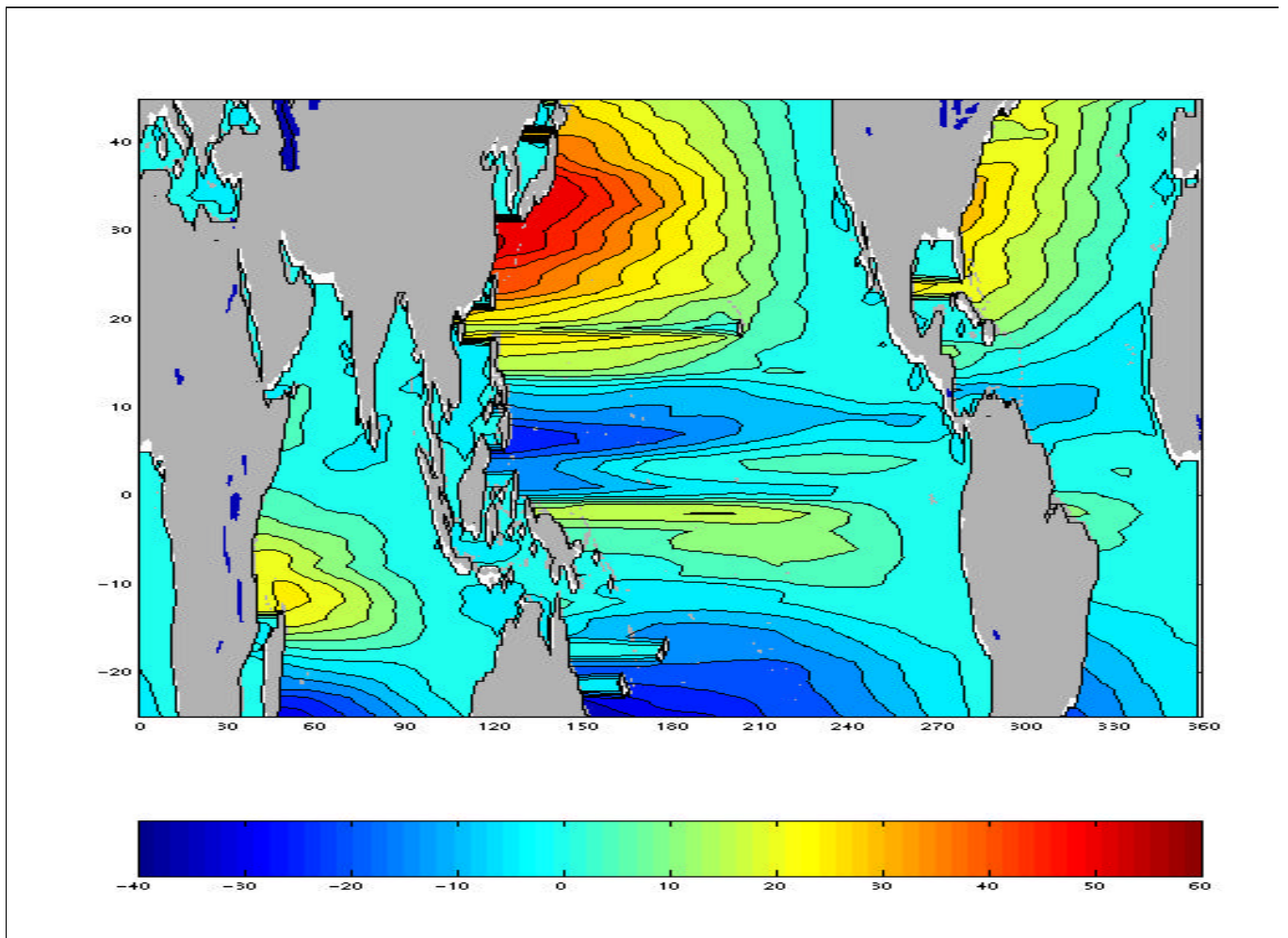


Figure 20

## Tables

Table 4 : Statistical parameters of daily QuikScat and NDBC buoy winds

Localisation	Variable	Bias	Std	Corr	Length
All	<i>W</i>	-0.33	1.57	0.89	5588
	<i>U</i>	-0.09	1.93	0.93	
	<i>V</i>	0.17	1.78	0.92	
	<i>Dir.</i>	5°	21°	-	
157.8°W, 17.2°N	<i>W</i>	-0.01	0.81	0.93	120
	<i>U</i>	0.92	1.96	0.71	
	<i>V</i>	-1.49	1.44	0.66	
	<i>Dir</i>	11°	8°	-	
85.9°W, 25.9°N	<i>W</i>	0.03	1.40	0.85	234
	<i>U</i>	0.08	1.85	0.91	
	<i>V</i>	-0.36	1.92	0.91	
	<i>Dir</i>	1°	20°	-	
131°W, 46.1°N	<i>W</i>	-0.11	1.20	0.95	150
	<i>U</i>	-0.40	1.71	0.95	
	<i>V</i>	0.27	1.74	0.94	
	<i>Dir</i>	5	17	-	
148.2°W, 56.3°N	<i>W</i>	-0.19	1.02	0.96	154
	<i>U</i>	-0.11	1.86	0.94	
	<i>V</i>	0.12	1.59	0.94	
	<i>Dir</i>	8	21		

Table 5 : Statistical parameters of daily QuikScat and TAO buoy winds

Localisation	Variable	Bias	Std	Corr	Length
All	<i>W</i>	-0.30	1.34	0.79	4896
	<i>U</i>	0.42	1.66	0.79	
	<i>V</i>	-1.12	1.50	0.87	
	<i>Dir.</i>	12°	15°	-	
180°E, 2°S	<i>W</i>	0.33	0.70	0.90	209
	<i>U</i>	0.38	0.83	0.89	
	<i>V</i>	-2.00	0.90	0.81	
	<i>Dir</i>	16°	8°	-	
170°W, 2°S	<i>W</i>	0.21	0.65	0.92	184
	<i>U</i>	-0.05	0.70	0.91	
	<i>V</i>	-0.69	0.87	0.81	
	<i>Dir</i>	5°	7°	-	
155°W, 2°S	<i>W</i>	0.43	0.84	0.87	162
	<i>U</i>	0.07	0.96	0.88	
	<i>V</i>	-1.42	0.83	0.83	
	<i>Dir</i>	11°	8°	-	
140°W, 2°S	<i>W</i>	0.12	0.82	0.84	103
	<i>U</i>	0.42	0.89	0.90	
	<i>V</i>	-1.38	1.01	0.86	
	<i>Dir</i>	13°	10°	-	
125°W, 2°S	<i>W</i>	-0.09	0.92	0.87	85
	<i>U</i>	0.92	1.32	0.85	
	<i>V</i>	-1.97	1.53	0.51	
	<i>Dir</i>	30°	18°	-	

## 7. References

- [1] NASA Quick Scatterometer, QuikSCAT Science Data Product, User's Manual, Overview & Geophysical Data Products, Version 2.0-Draft, Jet Propulsion Laboratory, California Institute of Technology, Doc. D-18053, May 2000
- [2] Weiss, B., Level 2B Data Software Interface Specification, QuikSCAT Era, SeaWinds Processing and Analysis Centre, Jet Propulsion Laboratory, California Institute of Technology, Doc. D-16079, May 2000
- [3] Bentamy A., P. Queffeulou, Y. Quilfen and K. Katsaros, 1999 : Ocean surface wind fields estimated from satellite active and passive microwave instruments, *IEEE Trans. Geosci. Remote Sensing*, 37, 2469-2486.
- [4] Beljaars, A.C.M, 1994 : The impact of some aspects of the boundary layer scheme in the ECMWF model. *Proc., Seminar on Parametrization of sub-grid scale processes*, Reading, UK, ECMWF, 125-161.
- [5] Smith S. D., 1988 : Coefficients for sea surface wind stress, heat flux and wind profiles as a function of wind speed and temperature. *J. Geophys. Res.*, 93, 15467-15472.



## 8. Contacts

The best source of information: CERSAT on Internet:

*<http://www.ifremer.fr/cersat/english>*

For more information on **CERSAT archiving and processing facility (FPAF)**, or **data access, file format and use**, please contact:

***Mr Jean-François PIOLLE***

CERSAT - IFREMER  
BP 70  
29280 PLOUZANE, France

Phone (33) 98-22-46-91  
Fax (33) 98-22-45-33  
Internet [fpaf@ifremer.fr](mailto:fpaf@ifremer.fr)

For more information on **QuikSCAT MWF product, processing details** or **data use**, please contact:

***Mr Abderrahim BENTAMY***

DRO/OS IFREMER  
BP 70  
29280 PLOUZANE, France

Phone (33) 98-22-44-12  
Fax (33) 98-22-45-33  
Internet  
[Abderrahim.Bentamy@ifremer.fr](mailto:Abderrahim.Bentamy@ifremer.fr)